Università degli Studi di Napoli Federico II

Facoltà di Ingegneria
*D*ipartimento di *I*nformatica e *S*istemistica

*T*esi di *D*ottorato di *R*icerca in Ingegneria Informatica ed Automatica
Novenbre 2010

Modelling and Control for Soft Finger Manipulation and Human-Robot Interaction

by

Fanny Ficuciello

Thesis Supervisor: **Prof. Luigi Villani**

Submitted to the Faculty of Engineering, University of Naples Federico II, in partial fulfillment of the requirements for the degree of Doctor of Philosophy.

Printed in Italy.
Napoli, November 2010.

Contents

Acknowledgements

I sincerely thank Prof. Luigi Villani for his support to the development of my research activities and for his constant availability.

It is a great pleasure to thank Prof. Bruno Siciliano for having transmitted me the passion for these studies. I thank you, Prof. Siciliano, for having trusted me and having let me undertake this important experience.

A special thanks goes to Prof. Stefano Stramigioli for having offered me the opportunity to come to the University of Twente in the Netherlands, where I have improved enormously my knowledge and my research skills.

Among the people who I met during my stay Prof. Raffaella Carloni deserves a special mentioning. She has been extremely helpful and constructing in advising my activity and she became a very good friend. I am especially grateful to Ludo Visser for his support, friendship, and enthusiasm in sharing his knowledge.

After all, I would like to thank my family and Francesco for their love and support. Finally, I would like to express my deep gratitude to my beloved friend Giuseppe who has incredibly changed me and the course of my life by helping me to grow and choose the way of freedom. I am eternally grateful to his 13 years of friendship and to his indelible teaching, he is always alive in my memory.

Fanny Ficuciello
November , 2010

Summary

One of the greatest challenges of humanoid robotics is to provide a robotic systems with autonomous and dextrous skills. Dextrous manipulation skills, for personal and service robots in unstructured environments, are of fundamental importance, in order to accomplish manipulation tasks in human-like ways and to realize a proper and safe cooperation between humans and robots.

The contributions presented in this thesis are aimed at modelling and controlling multi-fingered robotic hands with soft covers for manipulation tasks. The control issue of a hand-arm robotic system involved in grasping tasks, which can interact with the environment or a human, is also addressed.

A port-Hamiltonian model of a multi-fingered robotic hand, with soft-pads on the finger tips, grasping an object has been developed. The port-Hamiltonian framework is based on the description of systems in terms of energy variables, and their interconnection in terms of power ports. Any physical systems can be described by a set of elements storing kinetic or potential energy, a set of energy dissipating elements, and a set of power ports interconnected by power preserving interconnections. The viscoelastic behavior of the contact is described in terms of energy storage and dissipation. Using the concept of power ports, the dynamics of the hand, the contact, and the object are described. The algebraic constraints of the interconnected systems are represented by a geometric object, called Dirac structure. This provides a powerful way to describe the non-contact to contact transition and contact viscoelasticity, by using the concept of energy flows and power preserving interconnections. Using the port based model, an Intrinsically Passive Controller (IPC) is used to control the internal forces and the motion of the object.

In grasping tasks, in the case that also interaction with the environment or a human is involved, the control issue of a hand-arm robotic system, is addressed. The

control law adopted for the arm is a compliance object-level control, which aims to reduce the interaction forces. The control action is based on the reconstruction of the external load applied to the object, using the force sensors measurement at the fingertips. Force sensing is also used to compute in real time the desired contact forces, able to guarantee the stability of the grasp. The regulation of the grasping forces is in charge of the hand control.

In detail, the contents of the thesis are organized as follows.

- *Chapter 1* provides an introduction on grasping and manipulation applications in the context of advanced robotics where the robot has to operate in unstructured environment. Here the relevance of dexterous manipulation skills in performing many different tasks is emphasized. The framework of the research work in this section is introduced, i.e., the activities in the European project DEXMART. A brief description of the research objectives and the key innovations carried out within the DEXMART project are given.

- *Chapter 2* contains an overview on the relations between the designing features of a robotic hand and its anthropomorphism and dexterity. An overview on the best known robotic hands realized so far with the description of the main mechanical features is given as well. Then the robotic hand built within the DEXMART project is introduced. A detailed description of the mechanical structure and of the actuation system by means of tendons is provided. Moreover, the kinematics, the statics and the dynamics of the hand are derived. The control structure and the control of the interaction in presence of soft contact is analyzed.

- *Chapter 3* presents a port-Hamiltonian model of a multi-fingered robotic hand, with soft-pads, while grasping and manipulating an object. An introduction to the port-based formulation is provided. For the validation of the model, a simple example modeled in 20-sim simulation software is considered. Simulation results are presented to validate the model and to show the behavior of the system when an IPC based controller is applied.

- In *Chapter 4* the control issue of a hand-arm robotic system involved in grasping tasks, which can interact with the environment or a human, is addressed.

An introduction on the combined control of hand-arm systems is given. The proposed control action is based on the reconstruction of the forces applied to the object, using the measurement at the fingertips, in order to obtain a compliant behavior of the arm and to reduce the interaction forces. A detailed simulation model of the robotic hand has been developed with the aim of testing the control strategies, using the SimMechanics toolbox of MATLAB. Simulation tests in MATLAB/SimMechanics environment demonstrate the effectiveness of the proposed approach.

- *Chapter 5* contains concluding remarks and proposals for further investigations.

Chapter 1

Introduction

Dextrous manipulation skills, for personal and service robots in unstructured environments, are of fundamental importance in performing different tasks, in order to accomplish tasks in human-like ways and to realize a proper and safe cooperation between humans and robots. The robot of the future must be thought of heaving human excellence.

1.1 Grasping and Manipulation in Advanced Robotics

The robots currently on the market are employed mainly in industrial applications. The industrial automation systems, have characteristics of highly structured work environments. For this kind of applications, that do not require great features of autonomy, the technology can be considered now mature [17].

More recently, the interest of researchers has gradually moved toward a different type of robot: the robot called "advanced" or "autonomous." Advanced robotics is the science of robots with enhanced characteristics of autonomy, which work in unstructured or poorly structured environments, where there is also interaction with humans.

An industrial robot is basically a robotic manipulator that can take different positions and, equipped with a tool, can perform different operations with a preprogrammed movement through a computer and a series of motors. These manip-

ulators, operating in a completely known environment, have a limited capability of adaptation, through sensors, to the changes of the surrounding environment. In unstructured environments, which characterize the everyday life of human beings, performing a task, where the robot replaces humans or works in cooperation with them, can be very difficult and, above all, can not be planned a priori.

Indeed, if the working environment is not known, it is not possible to plan the action in detail, but only to give to the robot a "mission" to accomplish, providing maximum information on how the environment will be "changeable".

In addition the robot has to be equipped with a large number of sensors to directly acquire all the information necessary to operate, for example, to know where it is positioned in relation to a map, if there are fixed or moving obstacles in its path, where is the exact locations to be achieved, where are the dangerous areas, such as stairs. It must also have the ability to exploit and process this information in an intelligent way.

This problem is not simple and is related to the cognitive level of the robot, in the field of artificial intelligence. It is evident that, in order to finally use the robots in human environments, it should be considered that the cognitive and control level and the development of new technologies are aspects that influence each other.

The next generation of robots will coexist with humans and will interact with us physically. Recently, the 7th EU Research Framework Programme has been introduced, supporting research on the development and construction of robotic systems and other artificial cognitive systems than can process and interpret various kinds of sensor data, and act autonomously towards achieving goals, in dynamic real-life environments [27].

Among the project funded under the 7th EU Research Framework Programme there is the DEXMART project, that is the framework of my research activity. "DEXMART" is an acronym and stands for "DEXterous and autonomous dual-arm/hand robotic manipulation with sMART sensory-motor skills: A bridge from natural to artificial cognition".

The DEXMART project has the ambition to fill the gap between the use of robots in industrial environments and the use of future robots in everyday human and unstructured environments. The realization of a dexterous and autonomous dual-arm/hand manipulation system is still an open research issue. Bimanual ma-

nipulation is such a complex task combining different strategies, constraints, goals, advanced sensing and actuating technologies, requiring new concepts and design of artificial cognitive systems. The growing interest on robotic hands and robotic manipulation is because the next generation of robots will interact with people directly, and dexterous manipulation skills are necessary for this purpose. Domains of direct interaction are:

- Elderly-dominated society in industrialized countries.
- Desire of automatizing common daily tasks in homes and offices.
- Unmanned warfare with human augmentation.
- Assistance in heavy industrial jobs.
- Applications in hostile environments.
- People with disabilities and rehabilitation assistance.
- Medical and surgical applications.
- Entertainment and leisure applications.
- Aerospace applications.

Furthermore, the interest on manipulation is also due to recent studies about the relation between the intelligence of human beings and hands.

Nowadays, neuroscience, anthropology and philosophy converge in considering the activity of hand and touch as essential in the development of superior cognitive faculties like memory, imagination, language [47].

The hand has had a major role in the evolution of man. In fact, being able to use tools, humans have enabled a relationship to the world different from that of animals. Relationship between hand and mind, the two most distinguished features of humans among animals, has been discussed by the great philosophers since ancient times [11]. It is because humans had dexterous hands that they became intelligent, or the other way around?

Certainly the embodied characteristics of the human hand, like the motors, the sensors, the sensorimotor transformations and the constraints, influence learning

process, behavior, skills and cognitive functions, since human beings do not use hands only for grasping or manipulating objects but also for exploration, touch, perception of physical properties.

Therefore, the hand has a major role in the development and expansion of intelligence. On the other side, intellectual ability affect and determine the skill with which the hand is used.

There has been a revolution recently in neuroscience that concerns the synergies [54], which are a kind of alphabet with which our hands work and organize movements and that can be exploited to make a progress in technology.

Possible future applications for research related to those studies are prosthetic devices, robot hands that come into our homes and that may be more useful if they are capable hands, and finally haptic interfaces, i.e. interfaces that allow our hands to feel those feelings that the avatars feel in virtual reality in which they are immersed.

Therefore, if we want the robot to be part of our world, working with people and replacing them, we need robot manipulation capabilities similar to those of human beings. To make robots able to enter in this world of complex functions, we must understand how the relationship between the hand and the development of the intelligence is expressed. This can be a big step forward in the study and development of cognitive robotics. This study is part of the "Evolutionary Robotics".

Relying on more or less autonomous and intelligent robots offers safe improvement of human life and an improvement in society, both in terms of quality and efficiency. This is one of most critical issues in the design of robotic systems, and involve hight cognitive level and the control modalities, as well as the mechanical structure, the kinematic configuration, the actuation and sensing system.

The cognitive and control level and the development of new technologies are aspects that influence each other and will contribute to dexterous and autonomous manipulation capabilities of dual-arm/hand robotic systems.

The bio-mimetic approach is the preferred choice both for advanced actuation and sensing systems in order to make a robotic arm/hand system approaching the human in functionality and aesthetics.

This perspective moves inevitably a number of ethical issues. The presence of robots in homes and workplaces will inevitably lead to a change in habits and

lifestyle.

For these reasons, there is the need for an ethic that inspires the design, production and use of robots, taking into account the cultural, historical, and customs of different peoples and cultures. These are things that scientists can not and should not ignore. In this regard the "Roboethics", a newborn discipline dealing with problems related to the acceptability of new robotics technologies, is a useful tool to sensitize robotics researchers towards their responsibilities to society [63], [22].

1.2 Motivation and Thesis contribution

Since the next generation of robots will interact with people directly, the interest on the implementation of artificial systems to replicate the manipulating ability of the human hand is growing among researchers.

"Dexterity" and "anthropomorphism" are the main issues involved in the design and use of a robotic hand.

Dexterity denotes the capability of the end-effector to autonomously perform tasks with a certain level of complexity.

Anthropomorphism denotes the capability of a robotic end-effector to mimic the human hand in terms shape, size, aesthetic.

Those notion are widely discussed in the literature [11].

Besides the dexterity or the anthropomorphism, a desirable feature in the design of a robotic end-effector is the "integration". A right integration between mechanical parts, sensors and electronics systems and control algorithms is one of the most important concepts in the design of robotic devices in order to achieve structural simplification, increase of reliability, and drop of costs, moreover the dexterity and the functional capabilities of robot hands are the result of the integration of those contributions.

The kinematical configuration and the sensory equipment determine a potential dexterity intrinsically related to the hand structure. The potential dexterity of such a complex structure can be wasted if proper actuation or sensory system are not adopted and suitable control procedures are not implemented.

The emulation of the characteristics of humans, like soft tissues, the compliant behavior and structure, requires non-conventional approaches to the system design.

Moreover, the definition of the kinematic structure of the hand and of the fingers, the design of new types of sensors (position, force, torque, tactile) and their integration within the hand, the design of new actuators have an important role on the development of a new generation of dexterous robotic hands.

Integration concerns also the relation between the hand and the rest of the robotic system [7]. With the term of "modular hands" one consider the hand as an independent device to be applied at the end of an arm, the same hand can be applied to any kind of arm (i.e. the DLR Hands [14], the Barret Hand [31], the Salisbury's hand [53]). In the "integrated design hands" the hand is considered a non-separable part of the arm, deeply integrated with it, reproducing the biological model,(i.e. the Robonaut hand [2], the UB Hand [41]).

Control algorithms strictly depends on the mechanical structure and on the sensors available, viceversa, the use of suitable control strategies allows to use in a smart way the intrinsic properties of the hand, both for manipulation and for interaction with the environment, especially in cooperating tasks with humans. The control of the hand must ensure the application of suitable contact forces on the object through the fingers, able to held and move the object without slipping, reorienting it with respect to the palm or balancing the forces exchanged with the environment or humans.

The contributions presented in this thesis are aimed at modelling and controlling multi-fingered robotic hands with soft covers for manipulation tasks. The control issue of a hand-arm robotic system involved in grasping tasks, which can interact with the environment or a human, is also addressed. Due to the influence of mechanical parts, sensors and electronics systems in controlling a robotic hand, an overview on the relations between the designing features of a robotic hand and its anthropomorphism and dexterity, and an overview on the best known robotic hands realized so far by describing the main mechanical features is provided in Chapter 2. Since the framework of my activity is DEXMART, a large-scale integrating project which is funded under the European Community's 7th Framework Programme, the control issues addressed in my research are based on the characteristic of the robotic hand built within the DEXMART project [46].

A detailed description of the new hand developed by DEXMART research consortium, known as UB Hand III, and the mechanical structure and actuation system

by means of tendons is provided in the second part of Chapter 2 [5], [12], [8]. Moreover, the kinematics, the statics and the dynamics of the hand are derived and the control of the interaction in presence of soft contact is analyzed [9].

The modelling aspects concerning the interaction of the fingers with a manipulated object is addressed in Chapter 3. In detail, a port-Hamiltonian model of a multi-fingered robotic hand, with soft-pads, while grasping and manipulating an object [25] is presented. An introduction to the port-based formulation and to the advantages of using this framework is provided. For the validation of the model, a simple example modeled in 20-sim simulation software is considered. Simulation results are presented to validate the model and to show the behavior of the system when an IPC based controller is applied. The port-Hamiltonian framework is based on the description of systems in terms of energy variables, and their interconnection in terms of power ports. Any physical systems can be described by a set of elements storing kinetic or potential energy, a set of energy dissipating elements, and a set of power ports interconnected by power preserving interconnections. The viscoelastic behavior of the contact is described in terms of energy storage and dissipation. Using the concept of power ports, the dynamics of the hand, the contact, and the object are described. The algebraic constraints of the interconnected systems are represented by a geometric object, called Dirac structure. This provides a powerful way to describe the non-contact to contact transition and contact viscoelasticity, by using the concept of energy flows and power preserving interconnections.

The port-Hamiltonian approach has the potential to address the analysis and control from an energetic point of view and thus in a more immediate and intuitive way. Nevertheless, for complex robotic systems such as a robotic hand actuated by means of tendons and involving considerable problems of friction and elasticity, the use of this tool can be complex and difficult to implement. Thus for low level control problems applied to a complex structure like the hand of Bologna it is preferable to adopt the classical Lagrangian method for modeling and control, as addressed in the Chapter 4. It remains that the use of port-Hamiltonian method may be interesting for high-level control problems and where is expected the interaction with the environment, since the study can be addressed more intuitively using the concept of passivity.

The control issue of a hand-arm robotic system, in the case that interaction of

the grasped object with the environment or a human is involved, is addressed in Chapter 4 [26]. An introduction with a state of the art on the combined control of hand-arm systems is given. The control law adopted for the arm is a compliance object-level control, which aims to reduce the interaction forces. The control action is based on the reconstruction of the external load applied to the object, using the force sensors measurement at the fingertips in order to obtain a compliant behavior of the arm and to reduce the interaction forces. Force sensing is also used to compute in real time the desired contact forces, able to guarantee the stability of the grasp. The regulation of the grasping forces is in charge of the hand control. A detailed simulation model of the robotic hand has been developed with the aim of testing the control strategies, using the SimMechanics toolbox of MATLAB. Simulation tests in MATLAB/SimMechanics environment demonstrate the effectiveness of the proposed approach. Finally, in Chapter 5 concluding remarks and proposals for further investigations are provided.

Chapter 2

Robot Hands

The development of anthropomorphic robotic hands with high level of dexterity and mobility raises large number of technological issues. The emulation of the characteristics of humans, like soft tissues, the compliant behavior and structure, requires non-conventional approaches to the system design. Moreover, the definition of the kinematic structure of the hand and of the fingers, the design of new types of sensors (position, force, torque, tactile) and their integration within the hand, the design of new actuators with specified capabilities in terms of torques/velocities and given dimensions have an important role on the development of a new generation of dexterous robotic hands. A general overview of dexterous robotic hands is provided in this Chapter. Then, the new hand developed within the DEXMART project, which has been used for the control design, is presented with more details.

2.1 Overview on Robotic Hands

The designing features of a robotic hand are: number and kinematic configuration of the fingers, anthropomorphic or non-anthropomorphic aspect, built-in or remote actuation, transmission system (in case of remote actuation), sensor assignment, integration with a carrying device (robot arm) and control [57].

"Dexterity" and "anthropomorphism" are the main issues involved in the design and use of a robotic hand.

Dexterity denotes the capability of the end-effector to autonomously perform

tasks with a certain level of complexity.

Anthropomorphism denotes the capability of a robotic end-effector to mimic the human hand in terms shape, size, aesthetic, and is determined mainly by

- kinematics;
- smoothness of the contact surface;
- size and correct size ratio between the links.

The dexterity is a measure of hand capability of changing the configuration of the manipulated object from an initial configuration to a final one, arbitrarily chosen within the device workspace and divided in two main areas, i.e. grasping and internal manipulation.

Grasping is the capability of constraining objects in a fixed hand configuration such as the object is fixed with respect to the hand.

Internal manipulation is a controlled motion of the grasped object in the hand workspace, with the hand configuration changing with time.

The factors affecting dexterity are:

- morphological features;
- sensory equipment;
- control algorithms;
- task planning strategies.

Those notion are widely discussed in the literature [11].

Besides the dexterity or the anthropomorphism, a desirable feature in the design of a robotic end-effector is the "integration". A right integration between mechanical parts, sensors and electronics systems and control algorithms is one of the most important concepts in the design of robotic devices in order to achieve structural simplification, increase of reliability, and drop of costs, moreover the dexterity and the functional capabilities of robot hands are the result of the integration of those contributions. Integration concerns also the relation between the hand and the rest of the robotic system, [7].

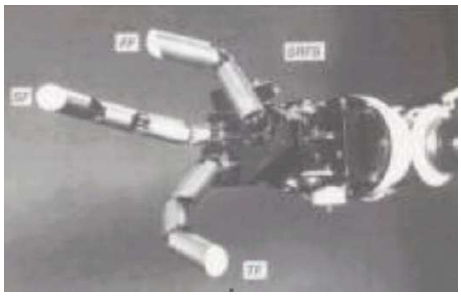

Figure 2.1: Okada Hand (1979).

With the term of "modular hands" one consider the hand as an independent device to be applied at the end of an arm, the same hand can be applied to any kind of arm (i.e. the DLR Hands [14], the Barret Hand [31], the Salisbury's hand [53]).

In the "integrated design hands" the hand is considered a non-separable part of the arm, deeply integrated with it, reproducing the biological model,(i.e. the Robonaut hand [2], the UB Hand [41]).

The kinematical configuration and the sensory equipment determine a potential dexterity intrinsically related to the hand structure. The potential dexterity of such a complex structure can be wasted if proper actuation or sensory system are not adopted and suitable control procedures are not implemented. Among the most known robotic hands one can mention in a chronological order: the Okada Hand (1979) [45], the Stanford/JPL Hand (1983) [53], the Utah/Mit Hand (1983) [24], the Barret Hand (1988) [65], [31], LMS Hand (1998) [30], the DIST Hand (1998) [16], [32], the Robonaut Hand (1999) [33], [40], the Tokyo Hand (1999) [38], the DLR-Hand II (2000) [14], the Tuat/Karlsruhe Hand (2000) [28], the Ultralight Hand (2000) [55], the Gifu Hand (2001) [37], the Shadow Hand (2002) [34], the UB Hand III (2010) [5].

2.1.1 Okada Hand

The Okada Hand (see Fig. 2.1) was built at the Electrotechnical laboratory in Japan in 1979. This is a modular hand composed by the two mail upper fingers and the opposable thumb and eleven joints all controlled, therefore eleven are the controlled degrees of freedom. The size is major than the human hand and the structural design is exoskeletal. The hand has a remote actuation with electrical revolute motor

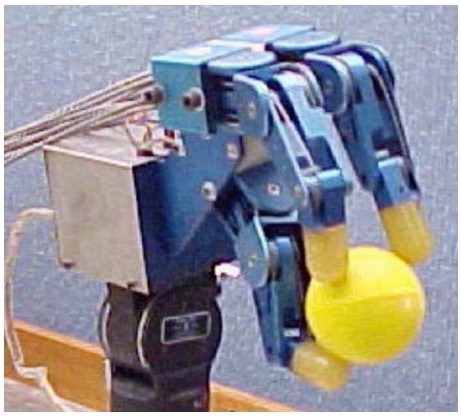

Figure 2.2: Stanford/JPL Hand (1983).

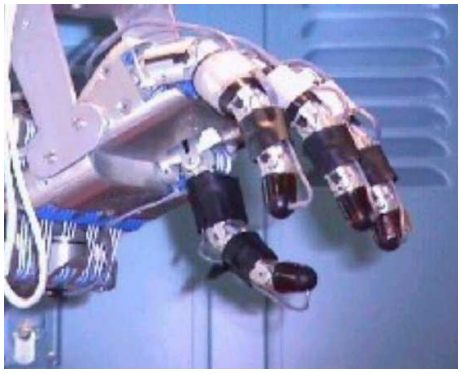

Figure 2.3: Utah Hand (1983).

by means of tendons transmission. The surfaces apt to contact with objects are fingertips and phalanges and are quite smooth and continue. The hand is equipped with motor and joint position sensors and motor effort sensors.

2.1.2 Stanford/JPL Hand

The Stanford/JPL Hand (see Fig. 2.2) was built at Stanford University in 1983. This is an integrated design hand. There are nine joints, all actuated, and three fingers. Only the fingertips are apt to contact with object, with a poor smoothness of the contact surface. The mechanical design is exoskeletal and the transmission is remote by means of tendons. The size is equal to the human hand. The hand is equipped with motor position sensors tendon tension sensors, moreover there are

Figure 2.4: Barret Hand (1998).

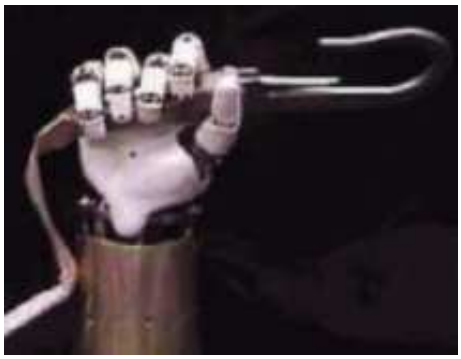

Figure 2.5: Robonaut Hand (1999)

fingertip tactile and force sensors.

2.1.3 Utah/Mit Hand

The hand (see Fig. 2.3) was built at Utah University in 1988, and it is constituted by four fingers and 16 joints, all controlled, in an integrated exoskeletal design. All the hand comprehensive of the palm is apt to contact with objects with a good smoothness. The size is equal to the human hand. The actuation is remote by means of tendon transmission and pneumatic actuators. Motor and joint position sensors, tendon tension sensors and tactile sensors are available.

Figure 2.6: DLR Hand II (2000)

2.1.4 Barret Hand

It is an underactuated hand built by Townsend in 1988 (see Fig. 2.4) constituted by three fingers with 8 joint, four of them are controlled. The structural design is exoskeletal, the actuation is inside the fingers with Brushless motors. The hand has motor position sensors and joint torque sensors. the contact surface smoothness is fair. The size is equal to the human hand.

2.1.5 Robonaut Hand

Among the endoskeletal hand there is the Robonaut hand (see Fig. 2.5) built at NASA Johnson Space Center in 1999. It is a five fingers hand with 22 number of joints and 14 number of controlled degrees of freedom. The whole hand with phalanges and palm is apt to contact with object with a very good contact surface smoothness. the actuation is remote with Brushless motors and flex-shaft transmission system.

The size is equal to the human hand. The hand is provided with tactile sensors, motor and joint position sensors and tendon tension sensors.

2.1.6 DLR Hand II

The DLR Hand II (see Fig. 2.6) has four fingers in an endoskeletal mechanical design with 17 joints and 13 number of controlled degrees of freedom. It is a modular hand,

Figure 2.7: Ultralight Hand (2000)

the actuation is inside the fingers and provided by electrical revolute motors. The non-actuated joints are rigid passive-driven joints. The transmission system is based on harmonic drives. The whole hand has a good contact surface smoothness. The hand has motor and joint position sensors and torque sensors at the joints, moreover a 6-axis force sensor is in the fingertip. The size is much bigger than the human hand.

2.1.7 Ultralight Hand

The Ultralight hand (see Fig. 2.7) was building at the Research center of Karlsruhe in 2000. It is an integrated exoskeletal design hand with 5 fingers and 18 joints. Only 13 joints are actuated. The whole hand has a good contact surface smoothness. The pneumatic actuation is inside the fingers and the non-actuated joints are rigid passive-driven joints. The size is much bigger than the human hand. The hand is provided of motor and joint position sensors and tactile sensors.

2.1.8 Gifu Hand

The Gifu hand (see Fig. 2.8) was built at Gifu University, it is a modular hand with five fingers and 20 joints, 16 of them are actuated with inside fingers actuation

Figure 2.8: Gifu Hand (2001)

system. The contact surface smoothness of the whole hand is good. The size is comparable with that of the human hand and the mechanical design is exoskeletal. there are motor position sensors and force and tactile sensors.

2.1.9 Shadow Hand

The Shadow hand (see Fig. 2.9) is an integrated design hand exoskeletal with a pneumatic remote actuation by means of tendon, it has 5 fingers and 23 joints all controlled. The contact smoothness is quite good. The hand is provided of motor and joint position sensors and motor effort sensor. The size is almost equal to that of the human hand.

2.2 DEXMART UB Hand III

The tendon-driven robotic hand, UB Hand III, biologically inspired has been developed by UNIBO [8]. The finger structure is realized by means of a fast prototyping, 3D printing process (see Fig. 2.10).

Apart from the sensors and electronics, the finger is entirely composed by

Fullcure®720. The great flexibility of the construction method allows to design the finger joints and the tendon pathways inside the phalanges structure with a level of precision and complexity difficult to obtain by means of conventional manufacturing. Tendons are the medium for transmitting forces in the new robotic hand

Figure 2.9: Shadow Hand (2002)

designed; this choice has been motivated by the easier mechanical production and assembly procures respect to the employment of other transmission methods.

Along with these advantages, the use of tendons causes some undesired effects as non linear frictional phenomena and plasticity.

2.2.1 Frictional phenomena

Despite the benefits achieved in terms of compactness, integration and simplified assembly, as a drawback, the mechanical structure is affected by a significant friction on both tendons and joints.

Frictional phenomena on the joints are due to the relative movement of two circular parts, one concave and the other convex, of two subsequent link pairs.

Moreover, tendon force transmission is affected by friction losses, due to the sliding of tendons along their pathways. Due to the relevance of these phenomena, a significant effort has been dedicated to model them.

Friction is a complex phenomena which is not easy to model. In [49] the different behaviors shown by static and dynamic friction models in the rendering of the friction phenomena acting on a tendon-based driving system have been evaluated. Satisfactory results were achieved using a Dahl friction model [21]. To further

Figure 2.10: First prototype of the robotic hand.

improve the fitting between simulation and experimental results, the LuGre dynamic friction model [21] has been adopted.

2.2.2 Actuator concept

The actuation system is based on the twisted string concept [66]. A module composed by four independent twisted strings, one for each finger tendon, has been built, and this module has been connected to the robotic finger (Fig. 2.11). In this way, each tendon can be independently actuated by means of a twisted string. A suitable solution to design the desired transmission compliance can be the introduction of compliant element directly integrated into the actuator. For this purpose, a compliant actuator has been designed, and their properties are under evaluation (Fig. 2.12).

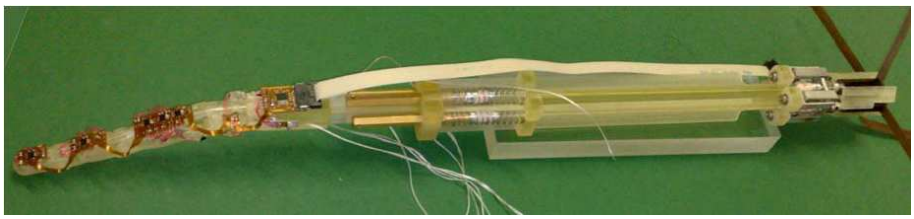

Figure 2.11: Robotic prototype finger with the actuation module based on the twisted string actuation.

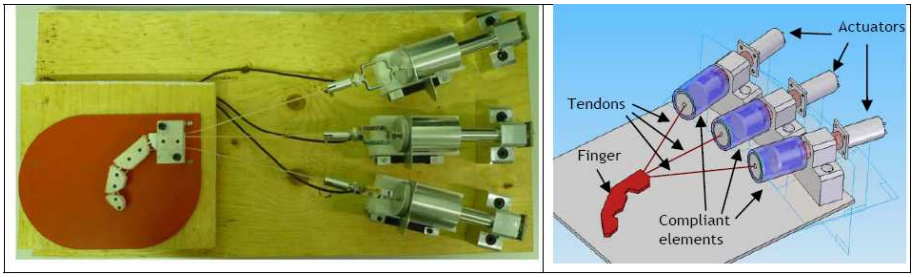

Figure 2.12: Picture and 3D drawing of the robotic finger with compliant actuation.

2.2.3 Sensors

The tactile sensor concept is based on the use of LED-phototransistor couples and a deformable elastic layer positioned above the optoelectronics devices [50]. This choice has been made to facilitate the integration into the robotic hand. The objective of the proposed sensor is to provide information about the contact point/area between the fingertips and the manipulated object, together with an estimate of both the normal and tangential components of the contact force.

A single joint of the robotic finger has been equipped with the displacement sensor that is based on a couple LED/photodiode, mounted to two contiguous phalanges of a UB hand finger [1].

For the measurement of the tendon force the combined use of the actuator side sensor and the finger side sensor will provide an accurate estimation of the actual joint torque needed for the finger control, overcoming negative effects of friction.

For the measurement of the tendon force at the actuation side has been developed two prototype sensor, one of them is based on a Fibre Bragg Grating (FBG) used as strain sensor and the other use a couple of optoelectronic components, an IR LED and a photodetector, mounted on a compliant structure that is deformed under the

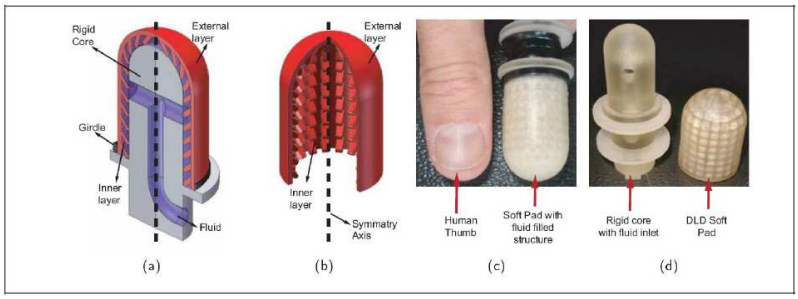

Figure 2.13: Fluid-filled soft pad concept and prototype. a) 3D model, b) longitudinal cross section, c) prototype comparison with human thumb dimensions, d) rigid core with fluid inlet and Differentiated Layer Design soft pad.

action of the tendon tension [18], [44].

2.2.4 Finger soft covers and contact modelling

A research activity has been focused on the realization of innovative covers with visco-elastic properties.

Alternatively to homogenous solid pads, has been proposed the use of fluid filled soft structures with Differentiated Layer Design [6]. This structure consists of a single solid material, dividing the overall thickness of the pad into a continuous skin layer coupled with an internal layer having communicating voids. The voids are then hermetically sealed and, in case, filled with fluid. The construction procedure depends on the pad material that is chosen. Two materials have been considered:

- Silicone rubber Wacker ELASTOSIL RT 623 A/B.
- Tango Plus Fullcure 930 (hardness 27 Shore A).

The proposed pad has several advantages namely: 1) less overall thickness; 2) predictable behavior; 3) possibility to alter the pad properties without losing surface continuity and adopted skin material. In the literature, different layers design have been studied and their behavior has been investigated.

Introducing a local compliance in the contact offers many advantages, namely, local shape adaptation to the object, extension of the contact area, and better energy dissipation in case of vibration and accidental interference. This leads to an improvement of contact stability and to a reduction of contact pressure and material

stress. Moreover, the safety in the interaction of the robot with human beings is improved.

The benefits of local compliance are described in [19], [56], [20]. Different design structures for the pad with shape and size similar to a human hand, and testing procedures to investigate properties and behavioral aspect have been presented in [29].

For the purpose of testing the interaction of the finger with a (rigid) environment, a pad model with an exponential relationship between the normal load and the flattering of the material has been chosen, i.e.:

$$N = \eta/\nu(e^{\nu\delta} - 1), \tag{2.1}$$

where N is the normal force, δ is the flattering of the soft pad in the normal direction, η and ν are constants determined from experimental tests. Consequently, the normal stiffness is

$$K_n = dN/d\delta = \eta e^{\nu\delta} = \nu N + \eta, \tag{2.2}$$

2.2.5 Finger kinematics

The finger has been designed following the human hand as a model; for this reason a tendon-actuated finger has been considered, where a coupling tendon (also referred as "passive tendon") is introduced to impose a coupling between the movements of the last two joints, similarity to the human hand.

The finger is constituted by a 4-DOF mechanical structure, whose kinematics (considering the fingertip position as end-point) is described by the Denavit-Hartenberg parameters summarized in Tab. 2.1.

The finger is actuated by means of four tendons: three agonistic tendons plus one antagonist tendon. An additional non-actuated tendon is used to couple the movements of the last two joints (medial and distal) inside the finger structure. This tendon configuration is known in literature as a "N+1" tendon network configuration [57], since all joints share an antagonist tendon. The tendons are fixed to the phalanges and routed inside the finger through suitable designed canals, as shown in Fig. 2.14. The tendon are constituted by FastFlight® cables: a complete analysis on the tendon transmission modelling, control and material selection is reported in [48].

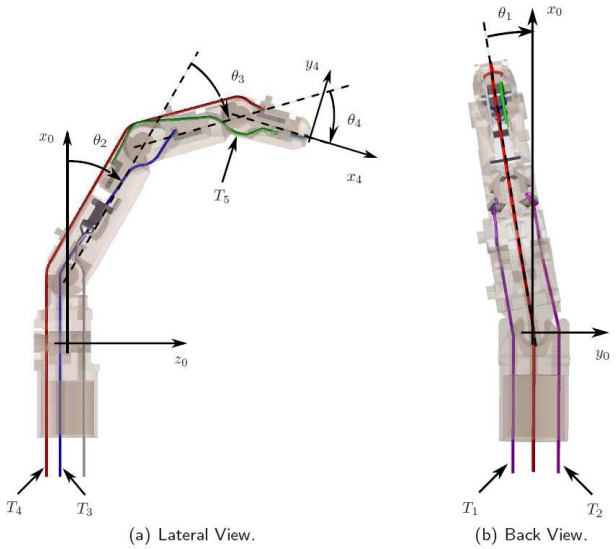

Figure 2.14: Tendon configuration and reference angles.

Tendon pathways have been designed so that tendons envelope on curved surfaces with constant radius along the entire joints movement range, leading to a linear relation between tendon and joint displacements.

Link	d	θ	a [m]	$\alpha[rad]$
1	0	θ_1	$a_1 = 20.2 \cdot 10^{-3}$	$\pi/2$
2	0	θ_2	$a_2 = 45.0 \cdot 10^{-3}$	0
3	0	θ_3	$a_3 = 29.9 \cdot 10^{-3}$	0
4	0	θ_4	$a_4 = 21.8 \cdot 10^{-3}$	0

Table 2.1: Denavit-Hartenberg parameters of the finger.

From the Denavit-Hartenberg parameters of the finger in Tab. 2.1, it is possible to compute the finger tip position $\mathbf{p}_{\text{eff}}$ with respect to the base reference frame:

$$\mathbf{p}_{\text{eff}} = \begin{bmatrix} C_1(a_1 + a_2C_2 + a_3C_{23} + a_4C_{234}) \\ (a_1 + a_2C_2 + a_3C_{23} + a_4C_{234})S_1 \\ a_2S_2 + a_3S_{23} + a_4S_{234} \end{bmatrix} \tag{2.3}$$

where C_{ijz} and S_{ijz} denote the functions $\sin(\theta_i + \theta_j + \theta_z)$ and $\cos(\theta_i + \theta_j + \theta_z)$, respectively. The joint angle ranges are mechanically constrained by stroke limiters

to intervals:

$$\theta_1 \in [-\pi/18,\, \pi/18], \quad \theta_{\{2,3,4\}} \in [0,\, \pi/2] \quad \text{[rad]} \tag{2.4}$$

Link 0 is the base of the finger (the hand palm). The other links, numbered from 1 to 4, correspond to abduction link, proximal, medial and distal phalanx respectively. The tendons are numbered from T_1 to T_5, as shown in 2.14:

- T_1, T_2: Tendons 1 and 2 drive the first two joints and are attached to link 2 (proximal phalanx).
- T_3: Tendon 3 drives the medial joint and is attached to the medial phalanx.
- T_4: Tendon 4 is the antagonist tendon, attached to the distal phalanx.
- T_5: Tendon 5 is the passive tendon connecting the proximal with the distal phalanx.

Due to the particular design and neglecting the tendon elasticity, the relation between the vector of the joint angles $\boldsymbol{\theta} = \begin{bmatrix}\theta_1 & \theta_2 & \theta_3 & \theta_4\end{bmatrix}^T$ and the vector of tendon displacements $\mathbf{l} = \begin{bmatrix}l_1 & l_2 & l_3 & l_4 & l_5\end{bmatrix}^{\mathbf{T}}$ can be considered linear, namely:

$$\mathbf{l} = \mathbf{H_c}\boldsymbol{\theta}, \qquad \mathbf{H_c} = \begin{bmatrix} r_{11} & r_{21} & 0 & 0 \\ -r_{11} & r_{21} & 0 & 0 \\ 0 & 0 & r_{33} & 0 \\ 0 & -r_{24} & -r_{34} & -r_{44} \\ 0 & 0 & -r_{35} & r_{45} \end{bmatrix}, \tag{2.5}$$

where r_{ij} is the radius of the circular surface that tendon i envelops on joint j. The numerical values of r_{ij} are reported in Tab. 2.2.

	r_{11}	r_{21}	r_{33}	r_{24}	r_{34}	r_{44}	r_{35}	r_{45}
radius [mm]	5.7	4.5	5.3	6.2	5.3	4.9	4.9	4.4

Table 2.2: Radii of the finger circular surfaces.

By considering $l_5 = 0$, i.e. assuming that the tendon T_5 is inextensible, the last equation in 2.5 gives the kinematic constraint imposed by the passive tendon:

$$\theta_4 = \frac{r_{35}}{r_{45}}\theta_3 \tag{2.6}$$

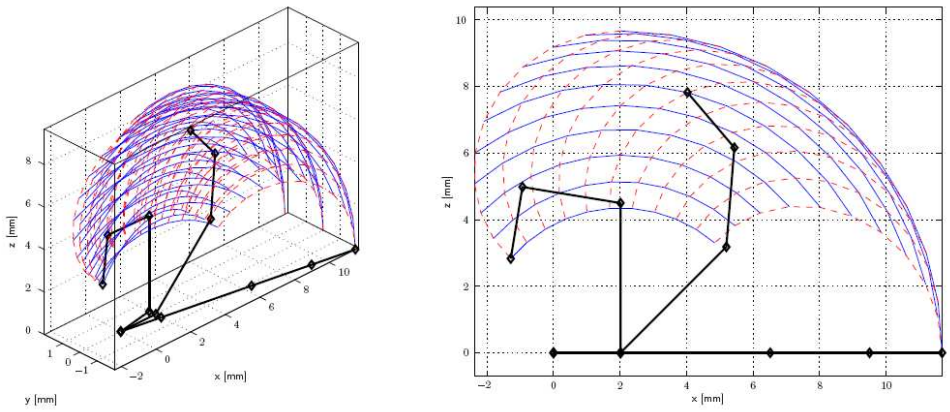

(a) 3d view (b) lateral view ($\theta_1 = 0$)

Figure 2.15: Finger workspace.

On the other hand, assuming that tendon T_5 has a linear elastic coefficient k_t and friction is negligible [48], from (2.5) it is possible to compute the relation between the force f_5 applied to the passive tendon and its elongation l_5:

$$f_5 = \begin{cases} -k_t l_5 = -k_t(\theta_3 r_{35} - \theta_4 r_{45}) & l_5 > 0, \\ 0 & l_5 \leq 0. \end{cases} \tag{2.7}$$

Obviously $l_5 \leq 0$ means that the tendon is slacking: this condition must be avoided by adopting a proper control strategy.

The finger workspace is shown in Fig. 2.15, assuming the constraint in Eq. (2.6).

In the simulation model of the finger, the actuators have been modeled as ideal force generators that impose the force vector $\mathbf{f^a} = \begin{bmatrix} f_1^a & f_2^a & f_3^a & f_4^a \end{bmatrix}^{\mathbf{T}}$.

2.2.6 Finger statics

The relation between the fingertip forces (see Fig. 2.16)

$$\mathbf{F} = \begin{bmatrix} F_x & F_y & F_z \end{bmatrix}^{\mathbf{T}}$$

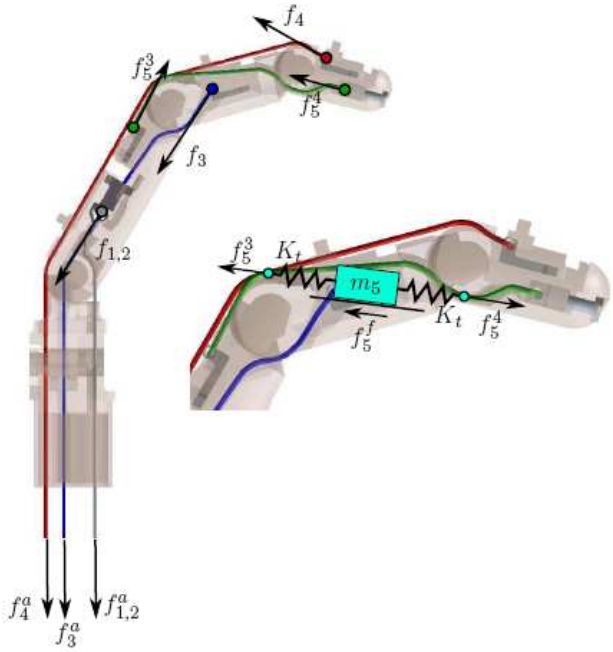

Figure 2.16: Schematic representation of the forces applied by the tendons on the finger and detail of the passive tendon implementation.

and the joint torques

$$\boldsymbol{\tau} = \begin{bmatrix} \tau_1 & \tau_2 & \tau_3 & \tau_4 \end{bmatrix}^T$$

is given by [58]:

$$\boldsymbol{\tau} = \mathbf{J^T F}, \quad \mathbf{J} = \frac{\partial \mathbf{p}_{\text{eff}}(\boldsymbol{\theta})}{\partial \boldsymbol{\theta}}, \tag{2.8}$$

where

$$\mathbf{J^T} = \begin{bmatrix} -(a_1{+}a_2C_2{+}a_3C_{23}{+}a_4C_{234})S_1 & C_1(a_1{+}a_2C_2{+}a_3C_{23}{+}a_4C_{234}) & 0 \\ -C_1(a_2S_2{+}a_3S_{23}{+}a_4S_{234}) & -S_1(a_2S_2{+}a_3S_{23}{+}a_4S_{234}) & a_2C_2{+}a_3C_{23}{+}a_4C_{234} \\ -C_1(a_3S_{23}{+}a_4S_{234}) & -S_1(a_3S_{23}{+}a_4S_{234}) & a_3C_{23}{+}a_4C_{234} \\ -a_4C_1S_{234} & -a_4S_1S_{234} & a_4C_{234} \end{bmatrix}. \tag{2.9}$$

Moreover, the relation between the tendon tension $\mathbf{f}$ and the joint torques $\boldsymbol{\tau}$ can be computed as [43]:

$$\boldsymbol{\tau} = \mathbf{H_c^T f}. \tag{2.10}$$

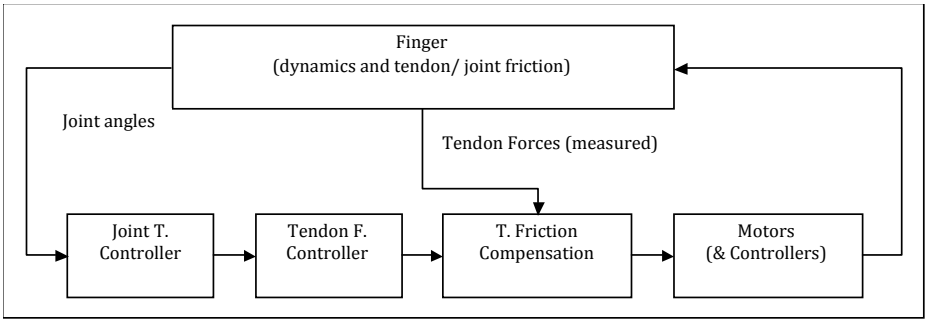

Figure 2.17: Schematic of the finger control structure.

Since the mappings (2.8) and (2.10) do not take into account the friction acting on both the tendons and the joints, the input force vector $\mathbf{f}$ is defined as

$$\mathbf{f} = \begin{bmatrix} f_1 & f_2 & f_3 & f_4 & f_5 \end{bmatrix}^{\mathbf{T}} \equiv \begin{bmatrix} f_1^a & f_2^a & f_3^a & f_4^a & f_5 \end{bmatrix}^{\mathbf{T}} \tag{2.11}$$

where the last element f_5 is given by 2.7.

2.2.7 Finger control structure

The control of the finger has to cope with friction and with the presence of the passive tendon, whose actuation force is not directly controllable, nor measurable, but depends on the relative configuration of the last two joints. Moreover, being the force transmitted by a tendon network, additional care must be taken in maintaining the tendons tensioned. The finger control system can be decomposed in three blocks (see Fig. 2.17):

- tendon friction compensation;
- tendon force controller;
- joint torque controller.

The tendon friction compensation is in charge of compensating tendon friction, using measurements of the tendon tension also to the finger side. The tendon force controller has as input the reference torques and as output the reference forces to motors that actuate the tendon network. The joint torque controller generates torque references in function of the chosen control strategies.

The first two blocks of the finger control structure are described with more details in the work developed by University of Bologna (see [48], [49]). The control interaction strategies implemented by the joint torque of the whole hand controllers will be illustrated in the following sections.

2.3 Hand Control

This Section reports the activities related to modelling and the control of the whole hand, designed following the human hand as a model.

A detailed simulation model of the robotic hand has been developed to test grasp control strategies, using a Matlab/Simulink simulation environment, based on the SimMechanics toolbox. The hand is constituted by five identical fingers, described in the previous Section.

In this Section, the hand kinematics of the DEXMART hand will be presented. Then, the complete dynamic model will be illustrated, together with the simulation results of the grasp control, based on the stiffness control.

2.3.1 Hand kinematics

The DEXMART hand (see Fig. 2.10) has twenty DOF's, due to the five fingers, assuming no extra DOF's in the palm. Due to the coupling between the last two joint of the fingers, only sixteen DOF's are linearly independent. Once the kinematics of every single finger is known, the kinematic model of the hand with respect to the palm can be easily computed on the basis of the constant homogeneous matrices corresponding to the coordinate transformations between the base frames of the five fingers and the palm frame.

The hand Jacobian depends on the vector of the fingers joint angles, given by the joint angles of the thumb and of the four fingers $\boldsymbol{\theta} = \begin{bmatrix} \boldsymbol{\theta}_t^T & \boldsymbol{\theta}_1^T & \boldsymbol{\theta}_2^T & \boldsymbol{\theta}_3^T & \boldsymbol{\theta}_4^T \end{bmatrix}^T$,

and has the form:

$$\mathbf{J_h} = \begin{bmatrix} \mathbf{J_t} & 0 & 0 & 0 & 0 \\ 0 & \mathbf{J_1} & 0 & 0 & 0 \\ 0 & 0 & \mathbf{J_2} & 0 & 0 \\ 0 & 0 & 0 & \mathbf{J_3} & 0 \\ 0 & 0 & 0 & 0 & \mathbf{J_4} \end{bmatrix} \tag{2.12}$$

where the matrices on the diagonal are the Jacobians of the thumb and of the four fingers. The expression of the Jacobian for the single finger is given in 2.9.

2.3.2 Hand dynamic model

The dynamic model of the whole hand composed by the four fingers and the thumb can be written in the classical Lagrange formulation as:

$$\mathbf{M_h}(\boldsymbol{\theta})\ddot{\boldsymbol{\theta}} + \mathbf{C_h}(\boldsymbol{\theta}, \dot{\boldsymbol{\theta}})\dot{\boldsymbol{\theta}} + \mathbf{g_h}(\boldsymbol{\theta}) = \boldsymbol{\tau}_\mathbf{h} - \boldsymbol{\tau}_\mathbf{h}^\mathbf{f} - \boldsymbol{\tau}_\mathbf{h}^\mathbf{r}(\boldsymbol{\theta}) - \mathbf{J}_\mathbf{h}^\mathbf{T}\mathbf{F_c} \tag{2.13}$$

where $\boldsymbol{\tau}_h$ is the vector of the joint torques, given by the vector

$$\mathbf{f_c} = \begin{bmatrix} \mathbf{f_t^T} & \mathbf{f_1^T} & \mathbf{f_2^T} & \mathbf{f_3^T} & \mathbf{f_4^T} \end{bmatrix}^\mathbf{T}$$

of the tendon forces of all the fingers, multiplied for an appropriate coupling matrix. Due to the presence of the tendon tension sensors, both in the motor and joint side, we can neglect low control problems, as tendon friction and elasticity, considering for control purposes directly the input $\boldsymbol{\tau}_h$. $\mathbf{M_h}(\boldsymbol{\theta})$ is the inertia matrix, $\mathbf{C_h}(\theta, \dot{\boldsymbol{\theta}})$ is the torque corresponding to Coriolis and centrifugal effects, $\mathbf{g_h}(\boldsymbol{\theta})$ is the vector of gravitational torques, $\boldsymbol{\tau}_h^f(\boldsymbol{\theta})$ is the vector of joint friction torques, $\boldsymbol{\tau}_h^r(\boldsymbol{\theta})$ is the reaction torque vector due to the presence of joint stroke limiters, and $\mathbf{F_c}$ is the vector of the contact forces deriving from the interaction with the object, namely $\mathbf{F_c} = \begin{bmatrix} \mathbf{F_t^T} & \mathbf{F_1^T} & \mathbf{F_2^T} & \mathbf{F_3^T} & \mathbf{F_4^T} \end{bmatrix}^\mathbf{T}$. $\mathbf{M_h}(\boldsymbol{\theta})$ and $\mathbf{C_h}(\boldsymbol{\theta}, \dot{\boldsymbol{\theta}})$ are diagonal matrices, whose diagonal element are the matrices of inertia and the Coriolis and centrifugal terms of each finger.

When the hand grasps an object, the dynamics of the object has to be considered as well. By adopting the classical Lagrange formulation, the equation of the object

can be written in the form [43]

$$\mathbf{M_0}(\mathbf{x_0})\ddot{\mathbf{x}}_\mathbf{0} + \mathbf{C_0}(\mathbf{x_0}, \dot{\mathbf{x}}_\mathbf{0})\dot{\mathbf{x}}_\mathbf{0} + \mathbf{g_0} = \mathbf{G}\mathbf{F_c} + \mathbf{F_{env}}, \tag{2.14}$$

where $\mathbf{F_{env}}$ is the force of the environment on the object and $\mathbf{x_0}$ is a vector representing the position and orientation of the object. $\mathbf{G}$ represents the grasp matrix, that is a linear map between the contact force, expressed in the contact frame, and the resultant force on the object $\mathbf{F}$, expressed in the object frame:

$$\mathbf{F} = \mathbf{G}\mathbf{F_c}.$$

When the fingers and the object are in contact, the dynamics of the two systems are coupled through the contact forces. Due to the presence of the soft-pad, these forces do not impose rigid constraints; thus, the number of generalized coordinates of the system is not reduced.

2.3.3 Hand grasp control

The complete dynamic model of the hand has been implemented in a Matlab/Simulink simulation environment, based on the SimMechanics toolbox; the model measurable outputs are the joint angle vector $\boldsymbol{\theta}$, and the contact forces of the fingertips with the object. Moreover, a block computing the forces deriving from the interaction of the tips with the objet, and a block corresponding to the object dynamics have been added. A soft finger contact type has been assumed for all the fingers.

The components of the contact forces exchanged between the soft fingers and the rigid object are computed according to a modified Hunt and Crossley model, that consists in a non-linear spring in parallel with a damper, with the following differential form:

$$F(t) = K\delta^n + D\delta^n\dot{\delta}, \tag{2.15}$$

where δ is the state of the spring, n is a parameter which depends on the material and the geometry taken into account and determined trough experiments. Here we have chosen $n = 1$. For the normal component of the contact force K has the expression in (2.2), and the elastic component is obtained from the expression

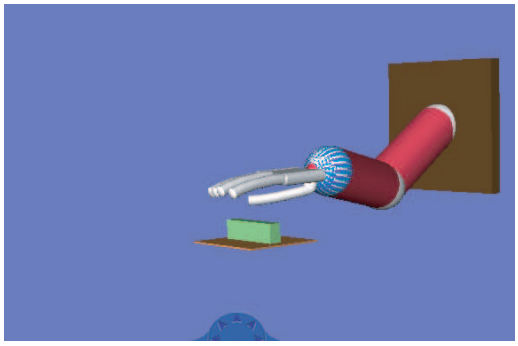

(a) Arm motion required to move the hand in a convenient pose for object graping

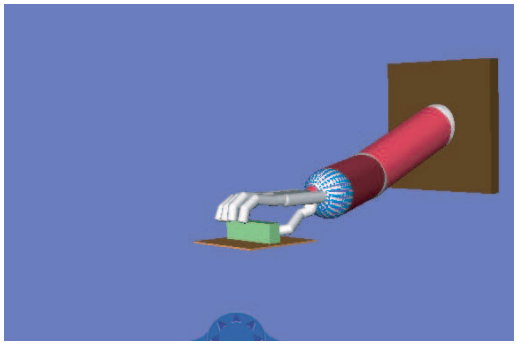

(b) Preshaping of the hand before grasping

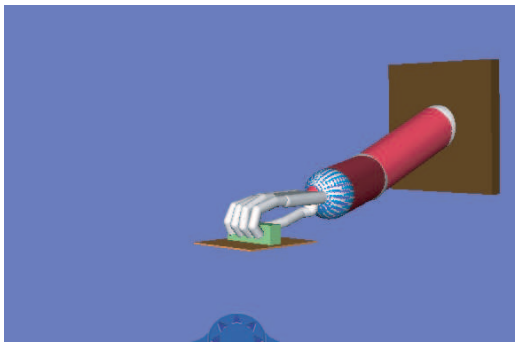

(c) Contact phase and regulation of the internal forces

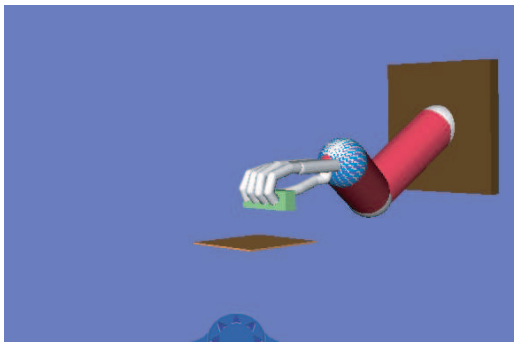

(d) Lifting phase of the object only by motion of the arm

Figure 2.18: Sequence of significant images.

$dN/d\delta_n = K_n$. This model, with different parameters, has been used for both the tangential and normal components of the contact force. The tangential component of the contact force is proportional to the tangential flattening of the soft pad trough the nonlinear tangential stiffness, $K_T(\delta_N)$, that depends on the normal displacement of the soft-pad.

Stiffness control

The stiffness control applied to a single finger has been extended to the whole hand, assuming that the position, the shape and the weight of the object are known. Once that the planner gives the optimal contact positions of each finger, using the grasp matrix $\mathbf{G}$ it is possible to know the amount of weight that every single finger has to balance. From the desired tangential components of the contact forces, the friction

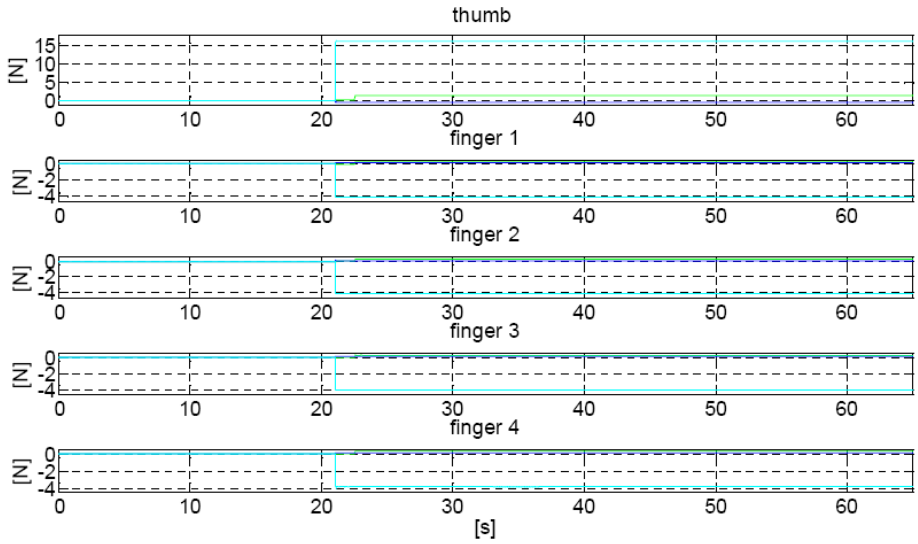

Figure 2.19: Cartesian components of the contact forces, normal component (red), Fx component (green),Fy component (blue).

cone conditions allow to compute the desired normal contact forces. By exploiting the exponential law of the soft-pad behavior between the contact force and the displacement of the pad, the desired position of the rigid part of the fingers can be computed. The control law for each finger in the case of cartesian space control is computed as

$$\boldsymbol{\tau}_d = \mathbf{J^T k_P}(\mathbf{p_d} - \mathbf{p_{eff}}), \tag{2.16}$$

where $\mathbf{J}$ is the Jacobian matrix, k_P is a positive scalar gain, while $\mathbf{p_d}$ and $\mathbf{p_{eff}}$ are the desired and actual position of the fingertip, respectively.

The executed task is described in 2.18, while the recorded data are reported in 2.19 and 2.20.

Notice that the fingers are not going in contact with the object at the same time, due to numerical problems, even if the planing is correctly designed. Consequently, there are non zero values of the tangential displacement of the soft-pad, even if the object weight is still balanced by the reaction force of the plane. When the hand raises the object, it is possible to notice the sudden increase in the tangential displacements of the soft pad and a slight variation of the normal displacement due to position errors.

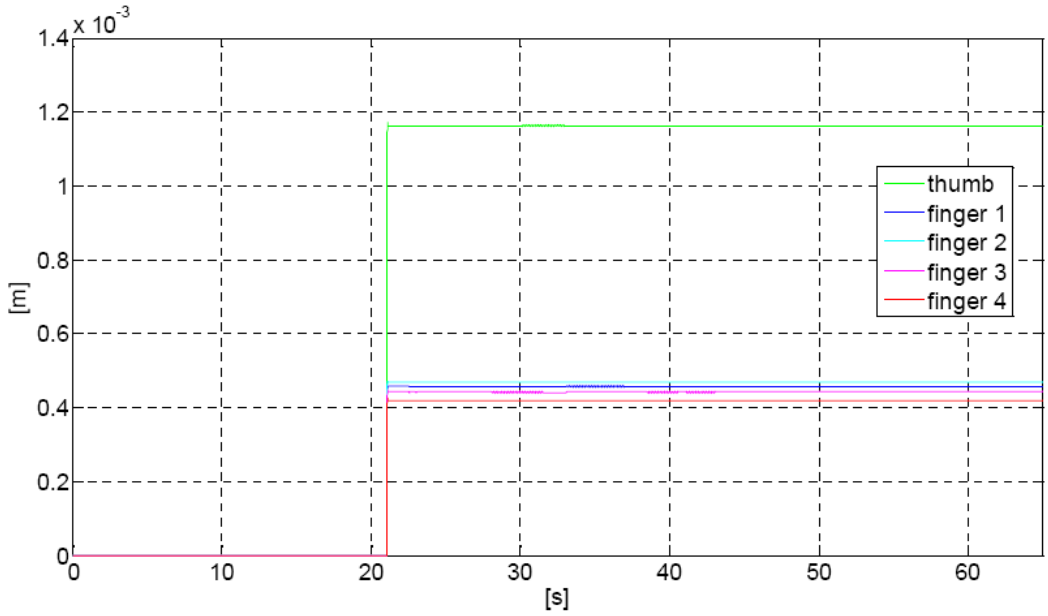

(a) Normal displacement of the soft pads

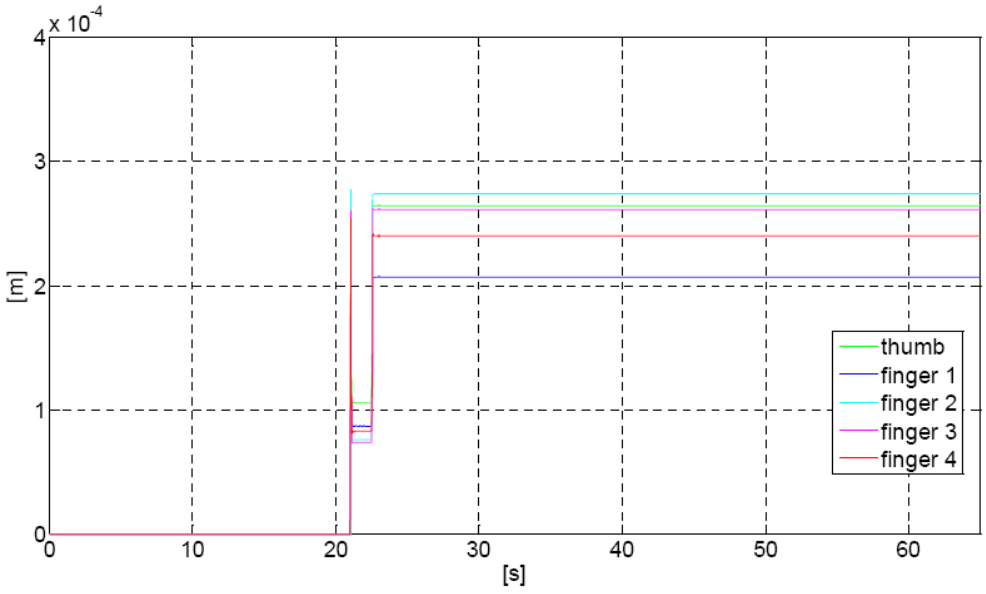

(b) Tangential displacement of the soft pads

Figure 2.20: Dynamic behavior of soft pads.

Chapter 3

Port-Hamiltonian Modelling for Soft-Finger Manipulation

Dextrous manipulation skills, for personal and service robots in unstructured environments, are of fundamental importance in performing different tasks.

Usually, a robotic hand has to manipulate objects of different shape, size, weight, material, and, in some cases, has to interact with human beings.

During manipulation, the dynamic properties of the controlled system change, due to the non-contact to contact transitions and due to the contact viscoelasticity. Therefore, in order to derive the dynamic model of a hand-object system during grasping, the contact model between the fingers and the object is of crucial interest.

In the Lagrangian formulation, the dynamic model of the hand-object system takes the form of a multibody system. In case of rigid contact, the whole system is a nonholonomic constrained system and the equations can be obtained using the Lagrange-DAlembert formulation, considering the grasping constraint equations [43].

In case of a compliant contact model, where the fingers have thick compliant layers of viscoelastic material, the grasping constraint equations are not valid anymore. Moreover, the dynamics of the contact are influencing the system dynamics, and have to be considered.

3.1 Port-Hamiltonian formalism

The port-Hamiltonian framework is based on describing a system in terms of energy variables and the interconnection of systems by means of power ports.

Any physical system can be described by a set of elements storing kinetic or potential energy, a set of energy dissipating elements, and a set of power preserving ports, through which energy can only be transferred and not produced [13]. The energy flow variables are intrinsically defined and are independent of the particular configuration of the physical systems.

The concept of a power port is an efficient and useful way to describe the interaction between physical systems and between the system and the environment.

The theory of port-Hamiltonian systems allows to describe the system behavior in a coordinate-free way and can be naturally extended to include constrained systems and compliant contact models.

This approach is useful to model and control the interaction between a robot and a passive environment.

The robot is a n-DOF mechanical passive system with respect to the controller, that can be modeled as a port-Hamiltonian system. To preserve a passive behavior in the interaction with the environment, both in case of contact and non-contact, an Intrinsically Passive Controller (IPC) [59], based on impedance control [35], can be used. Since the IPC approach yields an intrinsically passive system, the controlled system will be stable, both in case of contact and non-contact phases, for every passive, even unknown, environment. This is in contrast with a conventional hybrid controller, which switches from position to force control when a contact occurs. Such controllers can easily become unstable, because of noise affecting the force sensors that detect the contact. Moreover, a hybrid force/position control requires a perfect planning of the tasks, which is only possible if the environment is known.

In this work, a port-Hamiltonian model of a multi-fingered robotic hand, with soft-pads on the finger tips, grasping an object is presented.

The viscoelastic behavior of the contact is described in terms of energy storage and dissipation. Using the concept of power ports, the dynamics of the hand, the contact, and the object are described in a coordinate-free way.

Moreover, an IPC is applied to control the motion of the object and to regulate

the internal forces, i.e. the forces applied at the contact points and not influencing the object motion. These forces are important to have a stable grasp.

In the model of the hand-object system, we assume that the contact forces are always satisfying the friction cone conditions, i.e. the contact forces are always inside the friction cone, and we assume that there is no rolling contact. This means that the grasp matrix is constant.

The main advantage of the port-Hamiltonian formulation for constrained systems is that we do not need to modify the dynamic equations when a change occurs in the contact state. Instead, it is possible to represent both cases in a time-dependent geometrical structure, that satisfies the power continuity conditions in every contact state.

This framework allows to approach the problem in a more intuitive and compact way. The graphic bond graph representation of the system is based on the energy flow through the ports connecting the single components.

The port-Hamiltonian formalism has been introduced by van der Schaft and Maschke in [62]. Port-based modelling is at the basis of network theory, in which the different parts of the system are interconnected through power ports and described in terms of power exchange. A power port is defined by a pair of dual variables, a flow f and an effort e, whose intrinsic dual product $\langle e|f\rangle$ yields power. If $\mathcal{V}$ is the linear space of flows, then the dual space $\mathcal{V}^*$ is the linear space of efforts. On the space $\mathcal{V} \times \mathcal{V}^*$, it is possible to define a power continuous structure, called Dirac structure, which defines the interconnection between the power ports, i.e. it describes how the power is distributed between the ports. The Dirac structure is a subspace $\mathcal{D} \subset \mathcal{V} \times \mathcal{V}^*$ such that [61]:

$$\mathcal{D} = \{(f, e) \mid \langle e|f\rangle = 0, \quad \forall (f, e) \in \mathcal{D} \subset \mathcal{V} \times \mathcal{V}^*\}$$

A generic Dirac structure is depicted in Fig. 3.1. The bonds, connected to the structure, realize the ports through which energy can be exchanged with energy storage elements, energy dissipating elements, the controller, and the interaction port, with which the system interacts with the environment.

In order to derive the mathematical model of the manipulation system as a port-Hamiltonian system, we need to define a state manifold $\mathcal{S}$, of which the coordinates

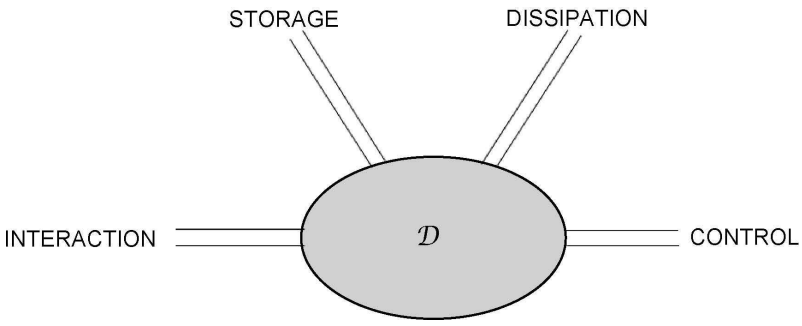

Figure 3.1: Dirac structure of a generic port-Hamiltonian system.

represent energy variables, and on $\mathcal{S}$ a Hamiltonian energy function $H : \mathcal{S} \to \mathbb{R}$ describing the total energy of the system. Then, by making explicit the Dirac structure, the system dynamics can be derived. Since an interconnection of port-Hamiltonian systems is again a port-Hamiltonian system, we can proceed by individually modelling the hand, the object that is manipulated, and the contacts, and to define the interconnection of the systems.

Regarding the Dirac structure of the contact model, observe that the contact represents the power continuous interconnection between the finger, the soft-pad and the object, in terms of elastic energy storage and energy dissipation. This interconnection can be represented considering the finger and the object as two rigid bodies connected trough a viscoelastic soft-pad. Since in a manipulation task both contact and non-contact situations may occur, the Dirac structure is not constant in time [52]. The contact and non-contact state are both represented in the same switching Dirac structure, which is, obviously, time dependent.

3.1.1 Problem statement

In the Lagrangian formulation, the dynamic model of a n-fingered hand, each with r degrees of freedom, has the form:

$$\mathbf{M}(\mathbf{q})\ddot{\mathbf{q}} + \mathbf{C}(\mathbf{q}, \dot{\mathbf{q}})\dot{\mathbf{q}} + \mathbf{g}(\mathbf{q}) = \boldsymbol{\tau} - \mathbf{J}_h^T \mathbf{W}_c$$

where $\mathbf{q} = \{\mathbf{q}_1, \ldots, \mathbf{q}_n\} \in \mathcal{Q}$ is the vector of the generalized configuration variables for the n fingers, with $\mathcal{Q}$ configuration manifold and $\dot{\mathbf{q}} \in T_q\mathcal{Q}$ their generalized

velocities, belonging to the tangent space of $\mathcal{Q}$ at $\mathbf{q}$. The vector $\boldsymbol{\tau} \in T_q^*\mathcal{Q}$ represents the generalized actuator forces at the joints, belonging to the co-tangent space of $\mathcal{Q}$ at $\mathbf{q}$. The matrix $\mathbf{J}_h$ is the hand Jacobian, that maps the joint velocities to the Cartesian fingertip velocities. From duality, it follows that the transpose $\mathbf{J}_h^T$ maps the fingertip forces to generalized joint forces. Let

$$\mathbf{W}_c = \{\mathbf{W}_{c_1}, \ldots, \mathbf{W}_{c_n}\} \tag{3.1}$$

be the vector of the contact wrenches.

The dynamics of the object are given by:

$$\mathbf{M}_0(\mathbf{x}_0)\ddot{\mathbf{x}}_0 + \mathbf{C}_0(\mathbf{x}_0, \dot{\mathbf{x}}_0)\dot{\mathbf{x}}_0 + \mathbf{g}_0(\mathbf{x}_0) = \mathbf{G}\mathbf{W}_c + \mathbf{F}_{\text{env}}$$

where $\mathbf{x}_0 \in \mathcal{X}$ represents the pose of the object, with $\mathcal{X}$ the configuration manifold of the object, and $\dot{\mathbf{x}}_0$ its generalized velocity.

To avoid singularities due to the local representation of the pose, we can describe the object dynamics globally by applying the Newton-Euler equations to the body configuration expressed in the Special Euclidian group $SE(3)$, and then obtain the Lagrange-D'Alembert representation choosing the local coordinates $\mathbf{x}_0 \in \mathcal{X}$ for the object configuration.

The matrix $\mathbf{G}$ is the grasp matrix, which is a linear map between the contact forces, expressed in the contact frame, and the resultant force on the object, expressed in the object frame [3].

The vector $\mathbf{G}\mathbf{W}_c$ describes the effect of the fingertip forces on the object, applied at the contact points. The external forces acting on the object are described by $\mathbf{F}_{\text{env}}$. In the hand and object dynamics, the matrices $\mathbf{M}(\mathbf{q})$, $\mathbf{M}_0(\mathbf{x}_0)$ are the symmetric and positive definite inertia matrices, the matrices $\mathbf{C}(\mathbf{q}, \dot{\mathbf{q}})$, $\mathbf{C}_0(\mathbf{x}_0, \dot{\mathbf{x}}_0)$ contain the centrifugal and Coriolis components, and $\mathbf{g}(\mathbf{q})$, $\mathbf{g}_0(\mathbf{x}_0)$ are the vectors of generalized gravity forces acting on the hand and the object, respectively [43].

In the context of Lie group theory, the relative configuration of two bodies can be studied using $SE(3)$. The relative instantaneous motion can be studied using the Lie algebra $se(3)$ associated to $SE(3)$, which is a 6D algebra, and corresponds to the six possible motions of a rigid body. The wrenches belong to the dual algebra

$se^*(3)$.

We assume that the fingers have thick compliant layers of viscoelastic material, and the dynamical behavior of the soft layers is modeled as a spring and a damper [10].

The model can be extended to a proper generalization to the full geometrical contact description, as proposed in [51].

In this work, we started from this geometrical analysis of the viscoelastic contacts between two objects without constraints, and extended this to a manipulation context, a complex multi-body system including the robotic hand, the soft-pads and the object and subject to constraints. The contact dynamics between the fingers and the object are represented with the same geometrical and energetically consistent model.

Moreover, a nonlinear Hunt-Crossley model of the contact is taken into account, for a better physical consistency and description of soft material behavior [23].

In Fig. 3.2, a schematic representation of the object and one finger in contact is shown. During the contact, a finger with soft-pad is able to transfer to the object four components of the contact wrench $\mathbf{W}_{ci}$, i.e. the three components of the linear contact force and the component of the contact torque around the direction orthogonal to the surface of the object in the point of contact.

Our goal is to describe the dynamics of this system in the port-Hamiltonian framework, including the contact dynamics. This allows to present the problem in a more intuitive and compact way. Moreover, given the port-Hamiltonian system representation, an IPC can be easily derived to control the system.

3.2 Contact model

In this Section, we derive the dynamic model of the contact, based on the Hunt-Crossley contact model [23]. The Hunt-Crossley model incorporates a spring in parallel with a nonlinear damper to model the viscoelastic dynamics.

In order to obtain a local representation of the Dirac structure of the contact in a matrix form, we have to define a contact frame in the contact point $\mathbf{c}_i$ on the object, as indicated in Fig. 3.2. The contact frame $\mathbf{\Sigma}_{ci}$ related to the finger i, has the origin in the contact point $\mathbf{c}_i$, and the axis z_{ci} is normal to the object surface,

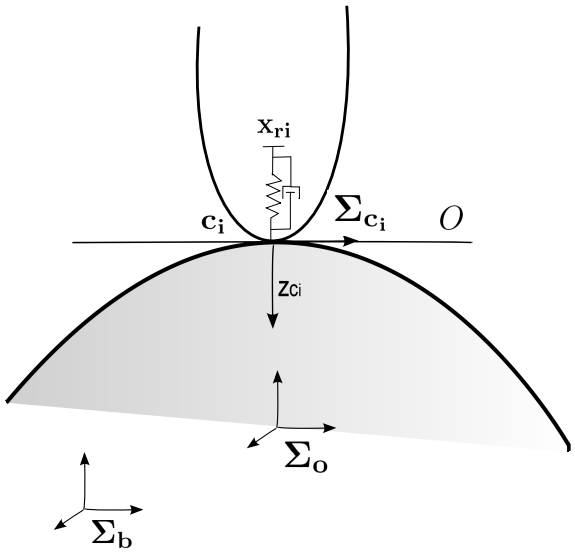

Figure 3.2: The geometrical contact model: the soft-pad is modeled as a spring and a damper according to the nonlinear Hunt-Crossley model.

pointing inside the object. There is a unique plane O orthogonal to z_{ci} and passing trough $\mathbf{c}_i$, spanned by the axis x_{ci} and y_{ci} of the contact frame. In Fig. 3.2, the object reference frame $\mathbf{\Sigma}_o$, and the world frame $\mathbf{\Sigma}_b$ are also depicted.

If we chose a basis of the two screws $(\mathbf{r}_x, \mathbf{r}_y)$, representing pure rotations around the two axes x_{ci} and y_{ci} of the contact frame, and a basis of the screws representing rotation around z_{ci} and the three translations $(\mathbf{r}_z, \mathbf{t}_x, \mathbf{t}_y, \mathbf{t}_z)$, we can decompose $se(3)$ in the direct sum of the two subspaces

$$S := \text{span } \{\mathbf{r}_z, \mathbf{t}_x, \mathbf{t}_y, \mathbf{t}_z\} \tag{3.2}$$

and

$$N := \text{span } \{\mathbf{r}_x, \mathbf{r}_y\}, \tag{3.3}$$

representing the subspace of the transferable wrenches in the contact point and the non transferable wrenches respectively. In particular, the motions in S involve a change in storage of potential energy in the viscoelastic contact [51].

A tangent map $\mathbf{P}$ exists, that projects a twists in $se(3)$ in the subspace S of

motions, and the dual cotangent map $\mathbf{P}^*$:

$$\mathbf{P} : se(3) \rightarrow S,$$

$$\mathbf{P}^* : S^* \rightarrow se^*(3).$$

Consequently, the elastic storage element, representing the elastic energy stored in the compressed surface of the soft-pad in contact with the object, is a 4D port with power variables $\bar{\mathbf{T}}_{r_i}^{c_i,c_i}$ and $\bar{\mathbf{W}}_{c_i,\text{store}^i}^{c}$, that are, respectively, the relative twist and the contact elastic wrench expressed in the contact frame and projected in the subspace of motions involving elastic storage of energy. In particular:

$$\bar{\mathbf{T}}_{r_i}^{c_i,c_i} = \mathbf{P}\,\mathbf{T}_{r_i}^{c_i,c_i}, \quad \mathbf{W}_{c_i,\text{store}^i}^{c} = \mathbf{P}^*\,\bar{\mathbf{W}}_{c_i,\text{store}^i}^{c}$$

Since the dynamics of the object are dependent of the set of all wrenches acting on it, it is necessary to measure the contact wrenches in order to compute the position of the object center of mass and of the points of contact.

Once the measurements of the contact wrenches are available, and the stiffness of the elastic storage element is known, the deformation (x, y, z, θ) of the soft-pad can be computed in the basis of the screws spanning the subspace of relative motions involving elastic storage of energy S.

Writing this deformation, relative to the contact coordinate frame, as an element $\bar{\mathbf{H}} \in SE(3)$:

$$\bar{\mathbf{H}} = \begin{bmatrix} \cos(\theta) & -\sin(\theta) & 0 & x \\ \sin(\theta) & \cos(\theta) & 0 & y \\ 0 & 0 & 1 & z \\ 0 & 0 & 0 & 1 \end{bmatrix}$$

the storage of potential energy in the element can be represented by a function

$$V(\bar{\mathbf{H}}) : SE(3) \rightarrow \mathbb{R}. \tag{3.4}$$

If $\bar{\mathbf{H}}(t)$ is known, the relative twist $\mathbf{T}_{r_i}^{c_i,c_i}$ of the object at the contact point with

respect to the finger i, can be expressed, in theory, in the contact frame as

$$\mathbf{T}_{r_i}^{c_i,c_i} = \dot{\bar{\mathbf{H}}}\bar{\mathbf{H}}^{-1}.$$

In practice we can obtain this twist by measuring the deformation of the soft-pad using and estimate the derivative using an observer or by numerical differentiation. The wrench generated due to a deformation $\delta\mathbf{T}_{r_i}^{c_i,c_i}$, related to the relative position of the rigid finger tip $\mathbf{x}_{r_i}^{c_i}$ and the object contact point $\mathbf{x}_{c_i}^{c_i}$, has the following expression in the contact frame, according to the Hunt-Crossley model[1]:

$$\mathbf{W}_{c_i}^{c_i} = \mathbf{K}_{s_i}\left(\delta\mathbf{T}_{r_i}^{c_i,c_i}\right) + \mathbf{D}_{s_i}\left(\delta\mathbf{T}_{r_i}^{c_i,c_i}\right)\mathbf{T}_{r_i}^{c_i,c_i} \tag{3.5}$$

where $\mathbf{K}_{s_i}$ is the two-covariant stiffness tensor [67], such that

$$\mathbf{K}_{s_i} = \mathbf{P}^*\bar{\mathbf{K}}_{s_i}\mathbf{P}$$

with $\bar{\mathbf{K}}_{s_i}$ the stiffness matrix that relates the 4D port variables $(\bar{\mathbf{T}}_{r_i}^{c_i,c_i}, \bar{\mathbf{W}}_{c_i,\text{store}}^{c_i})$, and $\mathbf{D}_{s_i}\left(\delta\mathbf{T}_{r_i}^{c_i,c_i}\right)$ is the damping matrix that depends on the deformation, and is defined locally as $\left(\delta\mathbf{T}_{r_i}^{c_i,c_i}\right)^T\mathbf{D}$, with $\mathbf{D}$ a constant diagonal matrix depending on the structure and on the material of the soft-pad.

By considering the map $\mathbf{P}^*$, we can express the vector of contact wrenches with respect to the contact deformation:

$$\mathbf{W}_{c_i}^{c_i} = \mathbf{P}^*\left(\bar{\mathbf{K}}_{s_i}\left(\delta\bar{\mathbf{T}}_{r_i}^{c_i,c_i}\right) + \bar{\mathbf{D}}_{s_i}\left(\delta\bar{\mathbf{T}}_{r_i}^{c_i,c_i}\right)\bar{\mathbf{T}}_{r_i}^{c_i,c_i}\right)$$

where $\bar{\mathbf{D}}_{s_i}$ is defined analogous to $\mathbf{D}_{s_i}$, but with respect to the 4D vector of the deformations:

$$\delta\bar{\mathbf{T}}_{r_i}^{c_i,c_i} = [x, y, z, \theta]^T$$

which represents the deformation of the soft-pad in the allowed directions.

[1] In the Hunt-Crossley model, the stiffness and damping forces are taken proportional to δ^m, with δ the scalar deformation and m usually close to unity. For simplicity, we have assumed $m = 1$ in this work.

3.3 Port-Hamiltonian model

In this Section, we intend to derive the port-Hamiltonian equations of the complete system. Therefore, starting from the general representation of Fig. 3.1, we can characterize the Dirac structure by explicitly describing the three different subsystems, i.e. the hand, the object and the contact. The complete system is composed by a number of storage and dissipative elements and interaction ports, connected together, as shown in Fig. 3.3.

The power port between the Dirac structure of the fingers and the Dirac structure of the contact is a multi-bond port.

In particular, the interconnection between the hand and the contact is identified by the effort $\mathbf{W}_{c_f}^b$, i.e. the vector of the wrenches exerted by the soft-pads (due to the object) on the fingers, and by the flow

$$\mathbf{T}_r^b = \mathbf{J}_h \dot{\mathbf{q}} \in \mathbb{R}^{6n},$$

i.e. the vector of the twists of the (rigid) finger tip in the base frame.

The power port between the Dirac structure of the object and the Dirac structure of the contact is a multi-bond port as well. The port is characterized by the effort $\mathbf{W}_{c_o}^b$, i.e. the vector of wrenches exerted by the fingers on the object, and by the flow

$$\mathbf{T}_c^b = \mathbf{G}^T(\mathbf{x}_0)\dot{\mathbf{x}}_0 \in \mathbb{R}^{6n},$$

i.e. the vector of the twists of the object in the contact points in the base frame.

The power port between the storage element of the soft-pads and the Dirac structure of the contact is characterized by the effort $\bar{\mathbf{W}}_{c,\text{store}}^c$, i.e. the vector of the wrench transferable component due to the (soft-pad) springs, represented by the vector of the partial derivatives of the total Hamiltonian energy function with respect to the vector of the states of the (soft-pad) springs, $\frac{\partial H}{\partial \mathbf{s}_c^T}$, and by the flow $\bar{\mathbf{T}}_r^{c,c} = \dot{\mathbf{s}}_c$, i.e. the vector of the relative twists between the fingers and the object, projected in the subspace S of the motion involving elastic storage of energy.

The power port between the dissipative element of the soft-pads and the Dirac structure of the contact is characterized by the effort $\bar{\mathbf{W}}_{c,\text{dis}}^c$, i.e. the vector of the wrench transferable component due to the (soft-pad) dampers, and by the flow $\bar{\mathbf{T}}_r^{c,c}$.

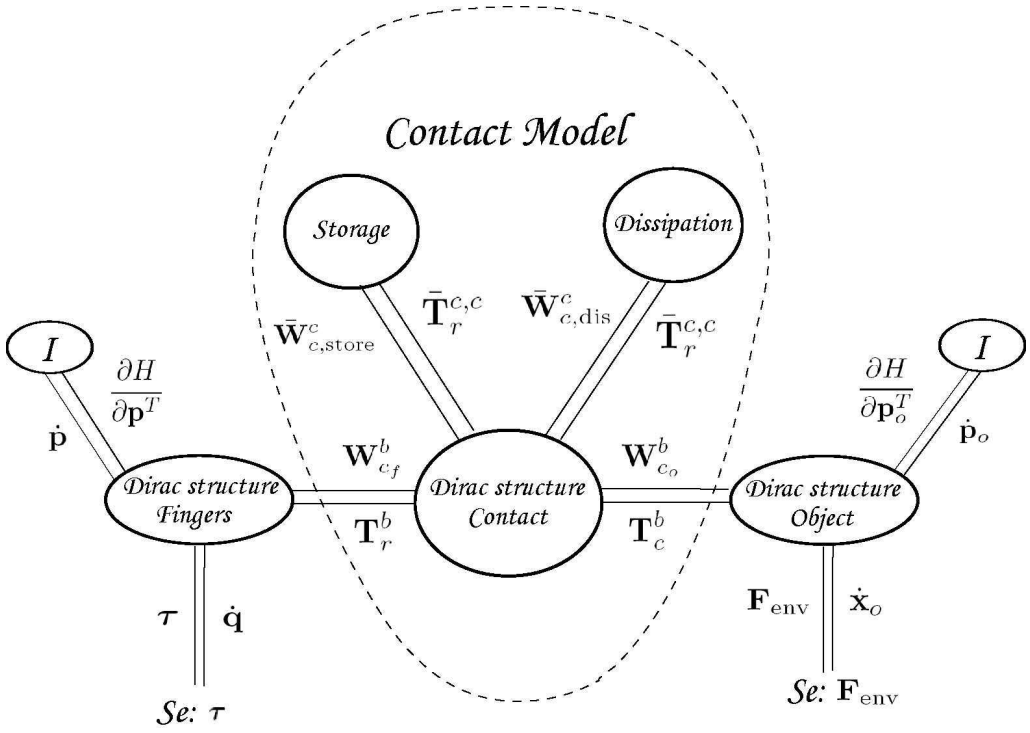

Figure 3.3: Dirac structure of the whole constrained port-Hamiltonian system. The fingers and the object are connected with two effort sources, that are, respectively, the control action and the external forces acting on the object.

To complete the description of the system represented in Fig. 3.3, we need to consider the inertia of the fingers, connected to the finger Dirac structure by means of the power flow defined by the conjugate variables $\left(\dot{\mathbf{p}}, \frac{\partial H}{\partial \mathbf{p}^T}\right)$, and the control port described by $(\dot{\mathbf{q}}, \boldsymbol{\tau})$.

For the object, we need to consider the inertia of the object, connected to the object Dirac structure by means of the power flow defined by the conjugate variables $\left(\dot{\mathbf{p}}_o, \frac{\partial H}{\partial \mathbf{p}_o^T}\right)$, and the environment interaction port described by $(\dot{\mathbf{x}}_o, \mathbf{F}_{\text{env}})$. For the sake of simplicity, we neglect Coriolis effects.

This simplification is justified because of the small work space we consider, and the relatively low velocities of the system.

For clarity, in the figure we have omitted the power port of the gravity external force, that we take in account in the port-Hamiltonian equations, for the fingers and the object, i.e. $\left(\dot{\mathbf{q}}_w, \frac{\partial H}{\partial \mathbf{q}^T}\right)$ and $\left(\dot{\mathbf{x}}_{o,w}, \frac{\partial H}{\partial \mathbf{x}_o^T}\right)$ respectively.

3.3.1 Dirac Structure of the fingers

The Hamiltonian energy function of the fingers is

$$H(\mathbf{s}_c, \mathbf{p}, \mathbf{q}) = \frac{1}{2}\mathbf{p}^T\mathbf{M}^{-1}(\mathbf{q})\mathbf{p} + \frac{1}{2}\mathbf{s}_c^T\bar{\mathbf{K}}_s\mathbf{s}_c + V(\mathbf{q})$$

where the first term is the kinetic energy of the finger, the second is the potential energy of the springs that model the soft-pads and $V(\mathbf{q})$ is the potential energy of the fingers due to gravity.

The Hamiltonian equations of the fingers are:

$$\dot{\mathbf{p}} = -\frac{\partial H}{\partial \mathbf{q}^T} + \mathbf{J}_h^T\mathbf{W}_{c_f}^b + \boldsymbol{\tau}, \quad \dot{\mathbf{q}} = \frac{\partial H}{\partial \mathbf{p}^T}$$

The Dirac structure can be represented by a skew-symmetric matrix:

$$\begin{bmatrix} \dot{\mathbf{p}} \\ \dot{\mathbf{q}} \\ \mathbf{T}_r^b \\ \dot{\mathbf{q}}_w \end{bmatrix} = \begin{bmatrix} \mathbf{0} & -\mathbf{1} & -\mathbf{J}_h^T & -\mathbf{1} \\ \mathbf{1} & \mathbf{0} & \mathbf{0} & \mathbf{0} \\ \mathbf{J}_h & \mathbf{0} & \mathbf{0} & \mathbf{0} \\ \mathbf{1} & \mathbf{0} & \mathbf{0} & \mathbf{0} \end{bmatrix} \begin{bmatrix} \frac{\partial H}{\partial \mathbf{p}^T} \\ -\boldsymbol{\tau} \\ -\mathbf{W}_{c_f}^b \\ \frac{\partial H}{\partial \mathbf{q}^T} \end{bmatrix}$$

where $\mathbf{0}$ and $\mathbf{1}$ denote zero and identity matrices of appropriate dimensions.

3.3.2 Dirac Structure of the object

The Hamiltonian energy function of the object is given by

$$H(\mathbf{p}, \mathbf{x}_o) = \frac{1}{2}\mathbf{p}_o^T\mathbf{M}^{-1}\mathbf{p}_o + V_o(\mathbf{x}_o)$$

where $V_o(\mathbf{x}_o)$ is the potential energy of the object due to gravity.

The Hamiltonian equations of the object are:

$$\dot{\mathbf{p}}_o = -\frac{\partial H}{\partial \mathbf{x}_o^T} + \mathbf{G}\mathbf{W}_{c_o}^b + \mathbf{F}_{\text{env}}, \quad \dot{\mathbf{x}}_o = \frac{\partial H}{\partial \mathbf{p}_o^T}$$

The Dirac structure can be represented by a skew-symmetric matrix:

$$\begin{bmatrix} \dot{\mathbf{p}}_o \\ \dot{\mathbf{q}}_o \\ \mathbf{T}_c^b \\ \dot{\mathbf{x}}_{o,w} \end{bmatrix} = \begin{bmatrix} \mathbf{0} & -\mathbf{1} & -\mathbf{G} & -\mathbf{1} \\ \mathbf{1} & \mathbf{0} & \mathbf{0} & \mathbf{0} \\ \mathbf{G}^T & \mathbf{0} & \mathbf{0} & \mathbf{0} \\ \mathbf{1} & \mathbf{0} & \mathbf{0} & \mathbf{0} \end{bmatrix} \begin{bmatrix} \frac{\partial H}{\partial \mathbf{p}_o^T} \\ -\mathbf{F}_{\text{env}} \\ -\mathbf{W}_{c_o}^b \\ \frac{\partial H}{\partial \mathbf{x}_o^T} \end{bmatrix}$$

3.3.3 Dirac Structure of the contact

In order to obtain a local representation of the Dirac structure of the contact in a matrix form, we have to choose a reference frame of the contact, and consider the transformation between the contact frame $\mathbf{\Sigma}_c$ and the world frame $\mathbf{\Sigma}_b$. In the case of soft finger contact model, the Dirac structure of the contact is the following:

$$\begin{bmatrix} \mathbf{W}_{c_f}^b \\ \mathbf{W}_{c_o}^b \\ \bar{\mathbf{T}}_r^{c,c} \\ \dot{\mathbf{s}}_c \end{bmatrix} = \begin{bmatrix} \mathbf{0} & \mathbf{0} & -\mathbf{A}^* & -\mathbf{A}^* \\ \mathbf{0} & \mathbf{0} & \mathbf{A}^* & \mathbf{A}^* \\ \mathbf{A} & -\mathbf{A} & \mathbf{0} & \mathbf{0} \\ \mathbf{A} & -\mathbf{A} & \mathbf{0} & \mathbf{0} \end{bmatrix} \begin{bmatrix} \mathbf{T}_r^b \\ \mathbf{T}_c^b \\ \bar{\mathbf{W}}_{c,\text{dis}}^c \\ \frac{\partial H_o}{\partial \mathbf{s}_c^T} \end{bmatrix}$$

where $\mathbf{A}^*$ is the matrix representation of the operator:

$$\mathbf{A}^* := \text{diag } \{\mathbf{A}_1^*, ..., \mathbf{A}_n^*\},$$

$$\mathbf{A}_i^* = (s_{\Delta,i} - 1)\text{Ad}_{\mathbf{H}_{bi}^c}^T \mathbf{P}^*$$

The matrix $\mathbf{A}$ is the dual operator to $\mathbf{A}^*$, and is expressed as the transpose of matrix expression for $\mathbf{A}^*$.

The binary signal $s_{\Delta,i}$ is defined as $s_{\Delta,i} = 1$ if there is no contact, and $s_{\Delta,i} = 0$ if there is contact [51]. If the position of the object is unknown, as in an unstructured environment, the binary signal can be related to the signal of a force sensor located in the soft-pad.

The adjoint operator $\text{Ad}_{\mathbf{H}_{bi}^c}$ transforms the relative twist between the rigid part of the finger i and the contact point on the object from coordinates in $\mathbf{\Sigma}_b$, the world frame, to $\mathbf{\Sigma}_{ci}$, the contact coordinate frame.

The first two equations give the expression of the contact forces acting on the

finger and on the object in case of contact and non-contact, thanks to the binary signal.

In case of non-contact they are zero and in the other case they are obviously opposite, and they have the expression of Hunt-Crossley model.

3.3.4 Dirac Structure of whole system

In this Section, we derive the Dirac structure of the whole system by combining the three Dirac structures derived for the different sub-systems. It follows that the skew-symmetric Dirac matrix is the following

$$\begin{bmatrix} \dot{\mathbf{p}} \\ \dot{\mathbf{q}} \\ \dot{\mathbf{q}}_w \\ \dot{\mathbf{p}}_o \\ \dot{\mathbf{x}}_o \\ \dot{\mathbf{x}}_{o,w} \\ \bar{\mathbf{T}}_r^{c,c} \\ \dot{\mathbf{s}}_c \end{bmatrix} = \begin{bmatrix} \mathbf{0} & -\mathbf{1} & -\mathbf{1} & \mathbf{0} & \mathbf{0} & \mathbf{0} & -\mathbf{J}_h^T\mathbf{A} & -\mathbf{J}_h^T\mathbf{A} \\ \mathbf{1} & \mathbf{0} & \mathbf{0} & \mathbf{0} & \mathbf{0} & \mathbf{0} & \mathbf{0} & \mathbf{0} \\ \mathbf{1} & \mathbf{0} & \mathbf{0} & \mathbf{0} & \mathbf{0} & \mathbf{0} & \mathbf{0} & \mathbf{0} \\ \mathbf{0} & \mathbf{0} & \mathbf{0} & \mathbf{0} & -\mathbf{1} & -\mathbf{1} & \mathbf{GA} & \mathbf{GA} \\ \mathbf{0} & \mathbf{0} & \mathbf{0} & \mathbf{1} & \mathbf{0} & \mathbf{0} & \mathbf{0} & \mathbf{0} \\ \mathbf{0} & \mathbf{0} & \mathbf{0} & \mathbf{1} & \mathbf{0} & \mathbf{0} & \mathbf{0} & \mathbf{0} \\ \mathbf{A}^T\mathbf{J}_h & \mathbf{0} & \mathbf{0} & -\mathbf{A}^T\mathbf{G}^T & \mathbf{0} & \mathbf{0} & \mathbf{0} & \mathbf{0} \\ \mathbf{A}^T\mathbf{J}_h & \mathbf{0} & \mathbf{0} & -\mathbf{A}^T\mathbf{G}^T & \mathbf{0} & \mathbf{0} & \mathbf{0} & \mathbf{0} \end{bmatrix} \begin{bmatrix} \frac{\partial H}{\partial \mathbf{p}^T} \\ -\boldsymbol{\tau} \\ \frac{\partial H}{\partial \mathbf{q}^T} \\ \frac{\partial H}{\partial \mathbf{p}_o^T} \\ -\mathbf{F}_{\text{env}} \\ \frac{\partial H}{\partial \mathbf{x}_o^T} \\ \bar{\mathbf{W}}_{c,\text{dis}}^c \\ \frac{\partial H}{\partial \mathbf{s}_c^T} \end{bmatrix} \tag{3.6}$$

and describes the energy flows through the system.

From Eq. (3.6) it is possible to obtain the input-state-output port-Hamiltonian system of the whole system.

The flow and effort variables of control and interaction port are split into conjugated input-output pairs.

The general form is the following:

$$\begin{aligned} \dot{\mathbf{x}} &= (\mathbf{J}(\mathbf{x}) - \mathbf{R}(\mathbf{x}))\,\frac{\partial H}{\partial \mathbf{x}^T} + \mathbf{g}(\mathbf{x})\mathbf{u} \\ \mathbf{y} &= \mathbf{g}^T(\mathbf{x})\frac{\partial H}{\partial \mathbf{x}^T} \end{aligned}$$

where $(\mathbf{u}, \mathbf{y})$ are the input/output pairs corresponding to the control port, the matrix $\mathbf{J}(\mathbf{x})$ is a skew-symmetric matrix representing the port topology defined by the Dirac

structure, while the matrix $\mathbf{R}(\mathbf{x}) = \mathbf{R}^T(\mathbf{x}) \geq 0$ specifies the energy dissipation. In our case we have the state

$$\mathbf{x} = \begin{bmatrix} \mathbf{p} & \mathbf{q} & \mathbf{p}_o & \mathbf{x}_o & \mathbf{s}_c \end{bmatrix}^T$$

and energy function

$$\begin{aligned} H(\mathbf{x}) &= \tfrac{1}{2}\mathbf{p}^T\mathbf{M}^{-1}(\mathbf{q})\mathbf{p} + \tfrac{1}{2}\mathbf{s}_c^T\bar{\mathbf{K}}_s\mathbf{s}_c + V(\mathbf{q}) \\ &\quad + \tfrac{1}{2}\mathbf{p}_o^T\mathbf{M}^{-1}\mathbf{p}_o + V_o(\mathbf{x}_o) \end{aligned}$$

Furthermore, we obtain:

$$\mathbf{J}(\mathbf{x}) = \begin{bmatrix} \mathbf{0} & -\mathbf{1} & \mathbf{0} & \mathbf{0} & -\mathbf{J}_h^T\mathbf{A} \\ \mathbf{1} & \mathbf{0} & \mathbf{0} & \mathbf{0} & \mathbf{0} \\ \mathbf{0} & \mathbf{0} & \mathbf{0} & -\mathbf{1} & \mathbf{GA} \\ \mathbf{0} & \mathbf{0} & \mathbf{1} & \mathbf{0} & \mathbf{0} \\ \mathbf{A}^T\mathbf{J}_h & \mathbf{0} & -\mathbf{A}^T\mathbf{G}^T & \mathbf{0} & \mathbf{0} \end{bmatrix}$$

$$\mathbf{R}(\mathbf{x}) = \begin{bmatrix} \mathbf{J}_h^T\mathbf{A}\bar{\mathbf{D}}\mathbf{A}^T\mathbf{J}_h & \mathbf{0} & \mathbf{J}_h^T\mathbf{A}\bar{\mathbf{D}}\mathbf{A}^T\mathbf{G}^T & \mathbf{0} & \mathbf{0} \\ \mathbf{0} & \mathbf{0} & \mathbf{0} & \mathbf{0} & \mathbf{0} \\ -\mathbf{GA}\bar{\mathbf{D}}\mathbf{A}^T\mathbf{J}_h & \mathbf{0} & \mathbf{GA}\bar{\mathbf{D}}\mathbf{A}^T\mathbf{G}^T & \mathbf{0} & \mathbf{0} \\ \mathbf{0} & \mathbf{0} & \mathbf{0} & \mathbf{0} & \mathbf{0} \\ \mathbf{0} & \mathbf{0} & \mathbf{0} & \mathbf{0} & \mathbf{0} \end{bmatrix}$$

$$\mathbf{g}(\mathbf{x}) = \begin{bmatrix} \mathbf{0} & \mathbf{1} & \mathbf{0} & \mathbf{0} & \mathbf{0} \\ \mathbf{0} & \mathbf{0} & \mathbf{0} & \mathbf{1} & \mathbf{0} \end{bmatrix}^T$$

$$\mathbf{u} = \begin{bmatrix} \boldsymbol{\tau} & \mathbf{F}_{\text{env}} \end{bmatrix}^T,$$

$$\mathbf{y} = \begin{bmatrix} \dot{\mathbf{q}} & \dot{\mathbf{x}}_o \end{bmatrix}^T$$

The matrix $\mathbf{J}(\mathbf{x})$ is obtained from Eq. (3.6) by inspection, as well as matrix $\mathbf{g}(\mathbf{x})$. The matrix $\mathbf{R}(\mathbf{x})$ is obtained considering the expression of the damping force in Eq. (3.5).

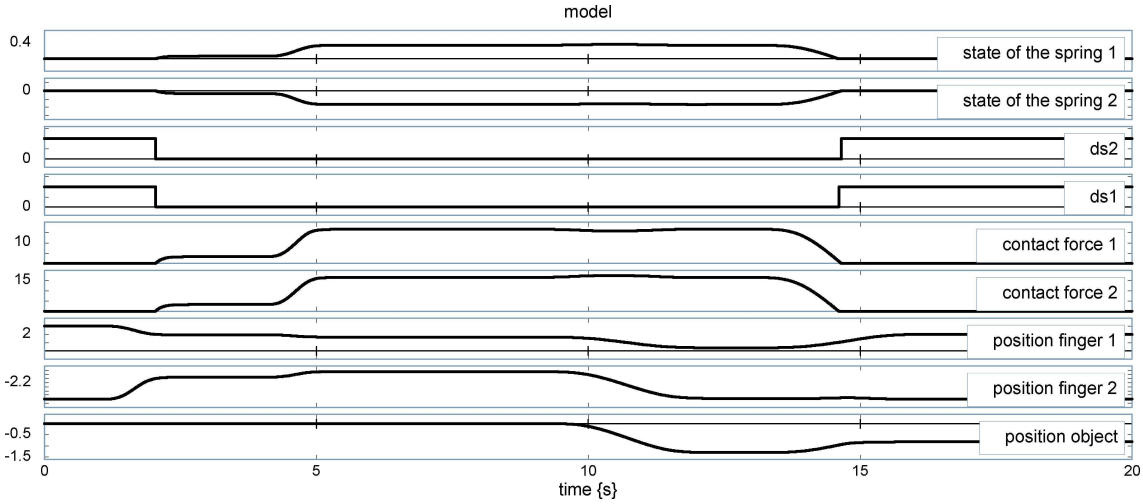

Figure 3.4: Simulation results - The simulations validate the model with control of the internal force and control of the object motion. When the binary signal switches from 1 to 0, the fingers are in contact with the object.

3.4 Simulations

For the validation of the model, a simple example modeled in 20-sim simulation software [15] is considered.

We implement the bond graph representation of two fingers with soft-pads, that interacts with an object in a plane.

An IPC is implemented to control the joint torques:

$$\boldsymbol{\tau} = \mathbf{g}(\mathbf{q}) + \mathbf{J}_h^T[\mathbf{K}_c(\mathbf{x}_{r_d} - \mathbf{x}_r)] - \mathbf{D}_c\dot{\mathbf{q}}$$

where the terms $\mathbf{K}_c$ and $\mathbf{D}_c$ are the proportional and derivative control gains. Here the desired rigid finger tips positions $\mathbf{x}_{r_d}$ are derived considering the desired forces at the contact and the model of the soft-pad.

By means of the virtual position, we are able to regulate the motion of the object and, through the null space of the grasp matrix, to regulate the internal forces as well by controlling the relative position of the finger tips. The soft-pad is modeled as a spring and a damper, with a stiffness constant $k = 50$ N/m, and damping constant $d = 3$ Ns/m. When the soft-pad touches the object, the binary signal s_Δ switches from 1 to 0.

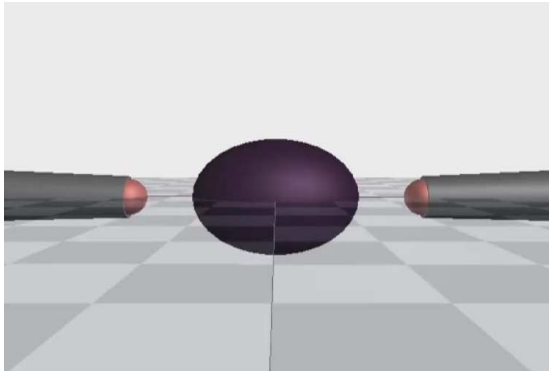

(a) The fingers move toward the object

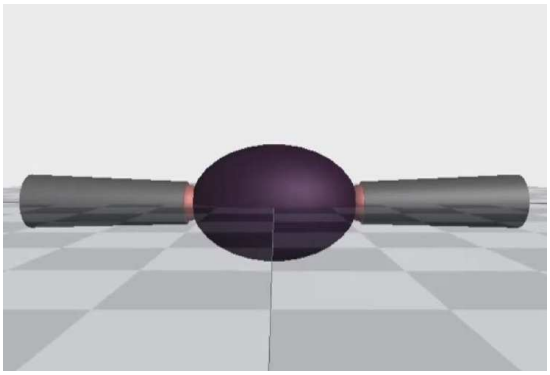

(b) The fingers push against the object to regulate the internal forces

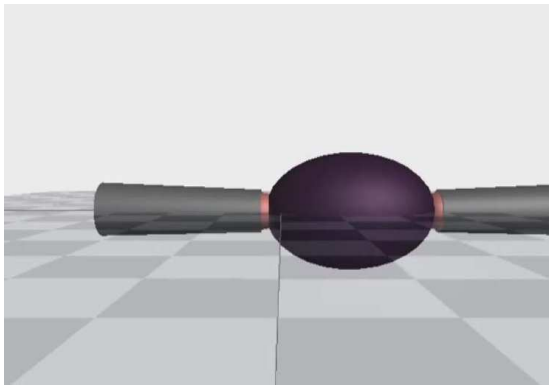

(c) The fingers move the object

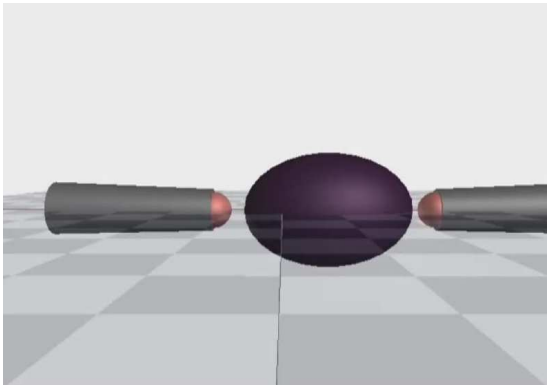

(d) The fingers release the object

Figure 3.5: Sequence of significant images.

The simulation is divided in three phases, see Fig. 3.5. First, the fingers move, touch the object and push against it until the internal forces are regulated at 16.5 N. Then, the fingers move the object, while maintaining the regulation of the internal forces at the same value.

The difference from the contact force of the two fingers are due to the inertia of the fingers and of the object. In the third step the fingers move away from the object. The object continues to move in the left direction, due to the deformation in the soft-pads, and it will stop due to the friction. Fig. 3.4 shows the diagrams of the positions of the finger tips and of the object, and the contact forces at the finger tips.

3.5 Concluding notes

The main advantage of port-Hamiltonian formalism is that it allows to describe the behavior of the system in terms of energy storage and energy flow, using the concept of power ports. Thus, its potential is to address the analysis and control from an energetic point of view.

Therefore, it is an useful way to describe the interaction between the object and the fingers, as well as the interaction of the whole system with the environment using the concept of passivity.

The drawback of this method is that for complex robotic systems the use of this tool can be complicated and difficult to implement. This is the case of the hand of Bologna where the actuation is by means of tendons and involve considerable problems of friction and elasticity. Thus for modeling and control the whole complex robotic system of UB hand III the classical Lagrangian method is adopted. The description of the finger control structure is addressed in Chapter 2 and the control of the whole hand-arm system during the interaction with the environment is addressed in the next Chapter.

Chapter 4

Impedance Hand-Arm Control for Human-Robot Interaction

In this chapter we present the control issue of a hand-arm robotic system involved in grasping tasks, which can interact trough the object with the environment or a human.

The control is in charge of ensuring that the hand firmly grasps and that the arm complies in the presence of external forces applied to the object.

These forces may require high values of the contact forces at fingertips, in order to have a stable grasp, that may saturate the hand actuators. To deal with this problem, the control law adopted for the arm is a compliance object-level control, which aims to reduce the interaction forces.

The control action is based on the reconstruction of the external load applied to the object, using the force sensors measurement at the fingertips.

Force sensing is also used to compute in real time the desired contact forces, able to guarantee the stability of the grasp. The regulation of the grasping forces is in charge of the hand control.

Simulation tests in MATLAB/SimMechanics environment demonstrate the effectiveness of the proposed approach.

4.1 Introduction and State of the Art

One of the greatest challenges of humanoid robotics is to provide a robotic hand-arm system with autonomous and dextrous skills. In order to accomplish the manipulation tasks in human-like ways and to realize a proper and safe cooperation between humans and robots, it is desirable to achieve a compliant behavior when interaction occurs.

Combined control of hand-arm systems has many issues of considerable complexity related to a stable and feasible grasp as a major goal and to the redundancy of the system. Moreover, in case of desired or undesired interaction of the grasped object with the environment, a stable grasp must be ensured while guaranteeing limited values of the interaction forces.

Most of the results in the field of interaction control of robot manipulators deal with serial-link open-chain structures. Actually, is not possible to consider a hand as a serial mechanical chain, instead is a redundant parallel device installed as an end-effector. Also, it should be noted that the hand and the arm have different behaviors and act in different ways, the previous is characterized by small motions and the latter by large motions, because different joint motions and velocities, as well as different inertia and kinematics are involved. In order to accomplish a given task, a simultaneous and coordinated motion of both the arm and the hand is required.

Many studies have been conducted in the past on the redundant hand-arm system dealing with the control and the planning of the whole device. A Jacobian transpose technique, is at the core of the method for the control of the hand-arm system including the partitioning of the contribution of the hand and the arm proposed in [42]. The theory was supported by simulations and experiments in the case of one finger attached to an arm.

An impedance control scheme for a 9-DOF finger-arm robot, combined with the steepest ascent method to modulate the manipulability of the finger, was proposed in [36]. Experiments demonstrate a good performance even when a dynamic external force is applied to the finger.

In the unified control scheme for a robotic arm-hand system proposed in [4], the complete dynamic model of the arm-fingers-object system is derived, and the control is designed by considering three superimposed tasks: internal force regulation,

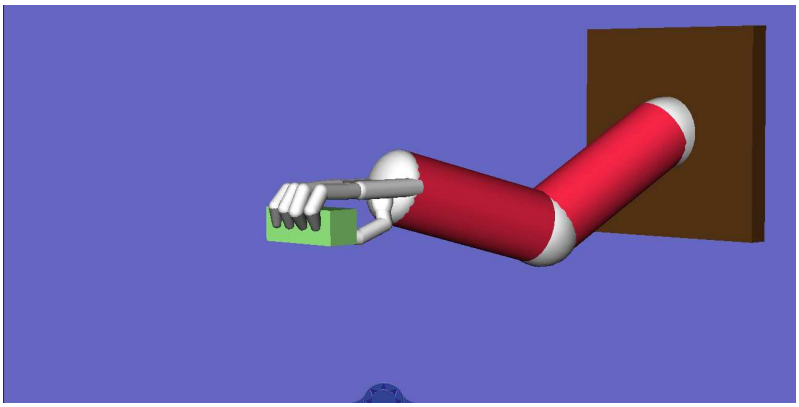

Figure 4.1: Rendering of the hand-arm-object system used in the simulation case study.

orientation control and position control of the grasped object.

An object-level impedance control for two-handed manipulation, based on the definition of a suitable potential function is considered in [64].

A hand-arm device has to interact physically with the environment, both with the grasped object and, through the object, with a human being or an obstacle. The main goal of the control is to ensure that the robotic hand do not lose the object and that the interaction forces with the environment are kept limited. Introducing a local compliance in the finger-tips offers many advantages, namely, local shape adaptation to the object, extension of the contact area, and better energy dissipation in case of vibration and accidental interference. This leads to an improvement of contact stability and to a reduction of contact pressure and material stress.

The benefits of local compliance are described in [19], [56], [20]. Different design structures for the pad with shape and size similar to a human hand, and testing procedures to investigate properties and behavioral aspects have been presented in [6].

In this work, we propose a control law for a hand-arm system with soft fingers for grasping tasks that involve also interaction with the environment. The rendering of the hand-arm-object system used in the simulation case study is shown in Fig. 1.

The load wrench (force and moment) acting on the object may change with time; consequently, the contact forces required to grasp and move the object has to be computed and imposed in real time by the controller.

The computation of the contact forces can be made using heuristic approaches in the simpler cases, or suitable real-time optimization procedures, in the case of objects of complex shapes or of complex tasks. Anyway, force measurements at the fingertips are essential to compute and impose the required contact forces.

For the purpose of control design, the hand and the arm are considered as two interacting but separate subsystems. The action of the external forces on the object may require very hight contact forces to maintain the grasp. These forces may produce torque saturation in the actuators of the hand.

To deal with this problem, a compliance object-level control is adopted for the arm, which aims at controlling the motion of the object while reducing the interaction forces with the environment, estimated on the basis of the forces measured at the fingertips. The regulation of the contact forces, required to guarantee the stability of the grasp, is in charge of the hand control.

4.2 Hand-Arm control

During the execution of a manipulation task, unexpected or pre-planned interactions of the object with the environment may occur. The main goal of the control is to ensure that the robotic system does not lose the object and that the exchanged forces remain limited. A crucial point is the control of the contact forces between the object and the fingers.

Keeping the contact forces within a certain range is important for several reasons. On the one hand, these forces must be sufficiently high to guarantee the satisfaction of the friction cone constraints; on the other hand, contact forces cannot be too high to avoid saturation of the motors and waste of energy, as well as to preserve the materials.

In this context, the presence of the force sensors at the fingertips plays an important role for the control of both the arm and the hand. In fact, an indirect measure of the external forces acting on the object can be achieved from the measure of the contact forces through the grasp matrix $\mathbf{G}$ [3]. This allows to adopt a compliant control strategy for the arm, that can be used both in free motion and in the presence of interaction. Moreover, using the contact forces measurements, it is possible to set these forces through the flattening of the soft pad, by controlling the

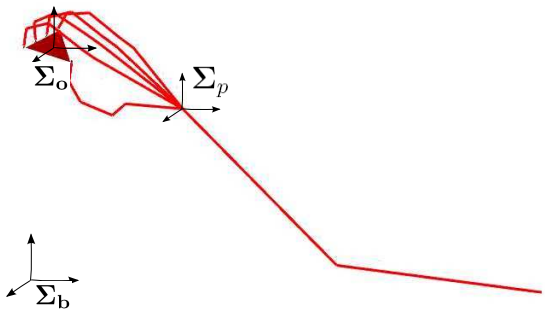

Figure 4.2: The figure represents a skeleton of the whole hand-arm-object system. The palm and object frames are represented.

position of the rigid part of the fingertips with respect to the palm. Hence, the same position control law can be adopted for the fingers during both the pre-grasping, the grasping and the manipulation phases.

Keeping a separate control for the arm and the hand lead to a better regulation of the internal grasping forces, which is in the charge of the finger control, while the interaction of the object with the environment or a human being is managed only by the arm control.

Moreover the separated control control laws of the hand and arm systems are efficient both in the pre-grasping and grasping manipulation phase.

4.2.1 Arm Control

In order to design the control law for the arm, a suitable frame fixed with respect to the arm must be selected. This can be the "palm" frame $\mathbf{\Sigma}_p$, namely, a frame fixed with respect to the palm of the multi fingered hand, see Fig. 4.2

The position and orientation of $\mathbf{\Sigma}_p$ with respect to the base frame $\mathbf{\Sigma}_b$ can be defined by a (6×1) pose vector $\mathbf{x}$, by adopting any kind of minimal representation of the orientation. Vector $\mathbf{x}$ depends only on the joint vector $\boldsymbol{\theta}$ of the arm through the direct kinematics equation, i.e., $\mathbf{x} = \mathbf{x}(\boldsymbol{\theta})$.

A compliant behavior to the arm can be ensured by using a simple PD with gravity compensation control law, assuming that a desired pose $\mathbf{x_d}$ is assigned to the arm, namely:

$$\boldsymbol{\tau}_a = \hat{\mathbf{g}} + \mathbf{J^T}(\boldsymbol{\theta})\mathbf{K_P}\boldsymbol{\Delta}\mathbf{x_p} - \mathbf{K_D}\dot{\boldsymbol{\theta}}, \tag{4.1}$$

where $\boldsymbol{\tau}_a$ is the vector of control torques for the arm, $\hat{\mathbf{g}}$ is a vector compensating the gravity torques acting on the arm and $\mathbf{K_P}$, $\mathbf{K_D}$ are positive definite matrix gains, that are usually set as diagonal. Vector $\Delta\mathbf{x_p}$ is a (6×1) pose error between the desired ($\mathbf{x_d}$) and actual ($\mathbf{x}$) pose of the arm, that can be defined in different ways for the orientation part, to ensure a physically consistent behavior in the presence of interaction with the environment.

Depending on the choice of $\Delta\mathbf{x_p}$, a proper Jacobian matrix $\mathbf{J}$ must be adopted in (4.1). In the following, for the sake of clarity, the problems related to the choice of the orientation error are ignored (since they require a significant complication of the analysis); hence, it is assumed that $\Delta\mathbf{x_p} = \mathbf{x_d} - \mathbf{x}$ and that $\mathbf{J}$ is the geometric Jacobian of the arm. As a further assumption, matrix $\mathbf{J}$ is non-singular.

It is well known that control law (4.1) ensures asymptotic stability of the equilibrium $\mathbf{x_d}$ (with null velocity), in the hypothesis of perfect gravity compensation and in free space.

On the other hand, when gravity compensation is imperfect, and in the presence of interaction with a passive environment, asymptotic stability can be still proven, but of a different equilibrium position $\mathbf{x_{eq}}$. The distance between $\mathbf{x_{eq}}$ and $\mathbf{x_d}$ depends on the gain $\mathbf{K_P}$: the lower $\mathbf{K_P}$, the higher the distance, with lower interaction force; this, in turns, means higher compliance of the arm.

The new equilibrium can be computed by considering the dynamic model of the controlled arm at steady state

$$\mathbf{g} + \mathbf{J^T}(\boldsymbol{\theta})\mathbf{h_{ext}} = \hat{\mathbf{g}} + \mathbf{J^T}(\boldsymbol{\theta})\mathbf{K_P}(\mathbf{x_d} - \mathbf{x}), \tag{4.2}$$

where $\mathbf{h_{ext}}$ is the external wrench (force and torque) acting on the arm, computed with respect to the origin of the palm frame $\boldsymbol{\Sigma}_p$.

The gravity vector $\mathbf{g}$ in (4.2) can be split into the sum of two contributions:

$$\mathbf{g} = \mathbf{g_{ah}}(\boldsymbol{\theta}, \mathbf{q}) + \mathbf{J^T}(\boldsymbol{\theta})\mathbf{h_{go}},$$

where $\mathbf{g_{ah}}$ is the gravity torque on the arm due to the weight of both arm and hand, depending on both arm ($\boldsymbol{\theta}$) and hand ($\mathbf{q}$) configurations, while $\mathbf{h_{go}}$ is the gravity wrench of the object, depending on the object weight and center of mass.

This wrench is mapped into the arm joint torques through matrix $\mathbf{J^T}$. Accordingly, vector $\hat{\mathbf{g}}$ can be split in the sum

$$\hat{\mathbf{g}} = \hat{\mathbf{g}}_{ah}(\boldsymbol{\theta}, \mathbf{q}) + \mathbf{J^T}(\boldsymbol{\theta})\hat{\mathbf{h}}_{\mathbf{go}},$$

with obvious meaning of the symbols.

The equilibrium equation (4.2) can be rewritten in the form [58]

$$\Delta\mathbf{h_{go}} + \mathbf{h_{ext}} = \mathbf{K_P}(\mathbf{x'_d} - \mathbf{x}), \tag{4.3}$$

with

$$\Delta\mathbf{h_{go}} = \mathbf{h_{go}} - \hat{\mathbf{h}}_{\mathbf{go}} \tag{4.4}$$

and

$$\mathbf{x'_d} = \mathbf{x_d} - \mathbf{K_P^{-1}}\mathbf{J^{-T}}(\mathbf{g_{ah}} - \hat{\mathbf{g}}_{\mathbf{ah}}). \tag{4.5}$$

In the case that force measurements are available, control law (4.1) can be modified as

$$\boldsymbol{\tau}_a = \hat{\mathbf{g}} + \mathbf{J^T}(\boldsymbol{\theta})(\mathbf{K_P}\boldsymbol{\Delta}\mathbf{x_p} - \mathbf{K_F}\hat{\mathbf{h}}_{\mathbf{ext}}) - \mathbf{K_D}\dot{\boldsymbol{\theta}}, \tag{4.6}$$

where $\hat{\mathbf{h}}_{ext}$ is an estimate of the external wrench acting on the object and $\mathbf{K_F}$ is a diagonal and positive definite matrix gain.

Notice that control law (4.6) coincides with (4.1) in the case $\mathbf{K_F} = \mathbf{0}$. The quantity $\hat{\mathbf{h}}_{ext}$ can be computed from the contact force measurements $\mathbf{F_c}$, by compensating the weight of the object, in the form:

$$\hat{\mathbf{h}}_{ext} = \mathbf{G_p}\mathbf{F_c} - \hat{\mathbf{h}}_{\mathbf{go}} = \mathbf{h_{ext}} + \boldsymbol{\Delta}\mathbf{h_{go}}, \tag{4.7}$$

where $\mathbf{G_p}$ is the grasp matrix referred to the origin of the palm frame $\boldsymbol{\Sigma}_p$. This equation holds at equilibrium, when the inertial contribution of the object is null. The new equilibrium for control law (4.6) now is:

$$\mathbf{g} + \mathbf{J^T}(\boldsymbol{\theta})\mathbf{h_{ext}} = \hat{\mathbf{g}} + \mathbf{J^T}(\boldsymbol{\theta})\left(\mathbf{K_P}(\mathbf{x_d} - \mathbf{x}) - \mathbf{K_F}\hat{\mathbf{h}}_{\mathbf{ext}}\right), \tag{4.8}$$

Using (4.7), the following equilibrium equation can be obtained with control

law (4.6)

$$\Delta \mathbf{h_{go}} + \mathbf{h_{ext}} = \mathbf{K_{PF}}(\mathbf{x'_d} - \mathbf{x}), \tag{4.9}$$

where $\mathbf{K_{PF}} = (\mathbf{I} + \mathbf{K_F})^{-1}\mathbf{K_P}$. Notice that, in the case $\mathbf{K_F} = \mathbf{0}$, control law (4.6) collapses into (4.1) and equilibrium equations (4.9) and (4.3) coincide.

The equilibrium pose $\mathbf{x_{eq}}$ can be computed by replacing the simple elastic law

$$\mathbf{h_{ext}} = \mathbf{K}(\mathbf{x} - \mathbf{x_e}), \tag{4.10}$$

into (4.9), being $\mathbf{K}$ the equivalent stiffness and $\mathbf{x_e}$ the undeformed pose of the environment. This leads to

$$\mathbf{x_{eq}} = (\mathbf{K} + \mathbf{K_{PF}})^{-1}(\mathbf{K_{PF}}\mathbf{x'_d} + \mathbf{K}\mathbf{x_e}) - (\mathbf{K} + \mathbf{K_{PF}})^{-1}\Delta \mathbf{h_{go}},$$

while the external force at equilibrium $\mathbf{x} = \mathbf{x_{eq}}$ has the expression

$$\mathbf{h_{ext}} = \mathbf{K}(\mathbf{K}+\mathbf{K_{PF}})^{-1}\mathbf{K_{PF}}(\mathbf{x'_d}-\mathbf{x_e}) - \mathbf{K}(\mathbf{K}+\mathbf{K_{PF}})^{-1}\Delta \mathbf{h_{go}}.$$

This last equation reveals that, when the arm interacts with a stiff environment (high values of $\mathbf{K}$), it is possible to reduce the interaction force by choosing low values of $\mathbf{K_{PF}}$ compared to $\mathbf{K}$. In fact, this produces

$$\mathbf{h_{ext}} \simeq \mathbf{K_{PF}}(\mathbf{x'_d} - \mathbf{x_e}) - \Delta \mathbf{h_{go}}.$$

On the other hand, when the arm moves free space ($\mathbf{h_{ext}} = \mathbf{0}$), the equilibrium pose is

$$\mathbf{x_{eq}} = \mathbf{x_d} + \mathbf{K_{PF}^{-1}}\Delta \mathbf{h_{go}} - \mathbf{K_P^{-1}}\mathbf{J^{-T}}(\mathbf{g_{ah}} - \hat{\mathbf{g}}_{\mathbf{ah}}), \tag{4.11}$$

revealing that, if the control law (4.1) is used (i.e., $\mathbf{K_{PF}} = \mathbf{K_P}$), a compliant behavior of the arm (low $\mathbf{K_P}$) can be achieved at the expense of a low position accuracy in free space.

On the other hand, with the control law (4.6), the compliance can be set choosing low values of $\mathbf{K_{PF}}$, while the position error due to the uncompensated arm/hand gravity can be recovered by setting high values of $\mathbf{K_P}$.

Notice that the last contribution of (4.11) may include also other non modelled

joint torques, as static friction, that can be considerably higher than the uncompensated gravity torques.

4.2.2 Hand Control

The hand control has the purpose of achieve the contact forces, $\mathbf{F_c}$, balancing the generalized external force acting on the object, that include object inertia and weight, and interaction forces with the environment. This is more clear observing the dynamics equation of the object:

$$\mathbf{M_0}(\mathbf{x_0})\ddot{\mathbf{x}}_\mathbf{0} + \mathbf{C_0}(\mathbf{x_0}, \dot{\mathbf{x}}_\mathbf{0})\dot{\mathbf{x}}_\mathbf{0} + \mathbf{h_0} = \mathbf{G}\mathbf{F_c} - \mathbf{h}_{\text{ext}} \tag{4.12}$$

where $\mathbf{x_0} \in \mathbb{R}^\mathbf{6}$ represents the pose of the object expressed in the base frame.

In this equation all the other terms are expressed in the base frame as well, due to the influence of the motion of the overall hand/arm system on the object dynamics.

$\mathbf{M_0}(\mathbf{x_0})$ is the symmetric and positive definite inertia matrix, the matrix $\mathbf{C_0}(\mathbf{x_0}, \dot{\mathbf{x}}_\mathbf{0})$ contain the centrifugal and Coriolis components, and $\mathbf{g_0}$ is the vector of generalized gravity forces acting on the object. The matrix $\mathbf{G}$ is the grasp matrix, which is a linear map between the contact forces, expressed in the contact frame, and the resultant force on the object, expressed in the base frame [3]. The expressions of every matrix terms, described before, are well known in the literature, [43].

The vector $\mathbf{GF_c}$ describes the effect of the fingertip forces on the object, applied at the contact points. The external generalized forces acting on the object are described by $\mathbf{h}_{\text{ext}}$ and, here, are expressed in the base frame.

Force measurements at the fingertips are essential to compute and impose the required contact forces. To avoid the slippage of the fingers on the object surface, each contact force has to be confined within the friction cone at the contact point.

Corresponding to the generic finger i, we indicate with $\mathbf{F_{N_i}}$ and $\mathbf{F_{T_i}}$ the normal and tangential component of the contact force $\mathbf{F_{c_i}}$.

The friction cone condition is given by the following scalar relation:

$$F_{T_i} \leq \mu F_{N_i}, \tag{4.13}$$

where μ is the friction coefficient depending on the materials in contact, that are supposed to be known.

The grasping force optimization problem consists in finding the set of contact forces balancing the generalized external force acting on the object, which are feasible with respect to the kinematic structure of the hand and to the corresponding joint torque limits, and minimize the overall stress applied the object, i.e, the internal forces, which are the forces applied at the contact points that not influence the object motion.

In this work we propose a simple example, with a prismatic object grasped with the four fingers on one side and the thumb in the other opposite side. By choosing the contact point positions on the object in a proper manner, in case of simple grasping task, the internal forces corresponds to the normal component.

In generic situation, which deal with irregular object or complex tasks, to find an optimal solution in real time of the grasping force optimization problem a well known algorithm, GFO [39], can be used.

Here to obtain in real time the desired contact forces, we solve locally the friction cone condition for each finger.

Among the infinite solution, we choose the ones that solve the following equation between the norms:

$$F_{N_i} = s/\mu F_{T_i}, \tag{4.14}$$

where F_{T_i} is meausured and s is a security coefficient to be chosen as a trade off between minimizing the contact forces and avoiding slippage in the case of vibration and accidental contact.

The solution of the previous equation is the desired normal force at the contact.

4.2.3 Finger Modelling and Control

To achieve the desired normal force, since each finger is covered by soft-viscoelastic layer, we consider the dynamic model of the contact based on the Hunt-Crossley model [23].

The Hunt-Crossley model incorporates a spring in parallel with a nonlinear damper to model the viscoelastic dynamics.

The elastic properties of the material has to be properly taken into account to model the interaction with the object.

An exponential relationship between the normal load and the flattening of the material has been chosen [29], i.e. in the normal direction to the object at the contact point:

$$F_N = \eta/\nu(e^{\nu\delta_N} - 1), \tag{4.15}$$

where F_N is the normal force component, δ_N is the flattening of the soft pad in the normal direction, η and ν are constants determined from experimental tests.

Consequently, the normal stiffness is

$$K_N = dN/d\delta_N = \eta e^{\nu\delta_N} = \nu N + \eta \tag{4.16}$$

If we want a desired force in the normal direction or a desired normal stiffness at the contact, we need to realize the desired flattening of the soft-pad, solving eq. (4.15) and (4.16), respectively.

Then, from the desired flattening of the soft pad is possible to compute the desired position of the rigid part of the finger tip (set point of the finger controller).

In order to compute the desired flattening of the soft-pad, we need to choose suitable reference frames at the contact, both for the finger and for the object.

Corresponding to each contact point i, the rigid fingertip and the object can be considered as two coupled rigid bodies with two attached reference frame, $\mathbf{\Sigma}_{ri}$ or $\mathbf{\Sigma}_{ci}$ respectively.

The object reference frame $\mathbf{\Sigma}_{ci}$, has the origin in the contact point $\mathbf{c_i}$ and the axis z_{ci} is normal to the object surface, pointing inside the object.

There is a unique plane O orthogonal to z_{ci} and passing trough $\mathbf{c_i}$, spanned by the axis x_{ci} and y_{ci} of the contact frame.

In this work rolling effect are neglected.

The finger frame, $\mathbf{\Sigma}_{ri}$ is supposed to be attached to a virtual point of the fingertip, such that at the equilibrium, in absence of the interaction forces, coincide with $\mathbf{\Sigma}_{ci}$.

Ideally, the model of the contact is a point contact model such that only forces can be exchanged between the finger and the object.

The finger has one abduction joint and two flection joints, with 3-DOF in the

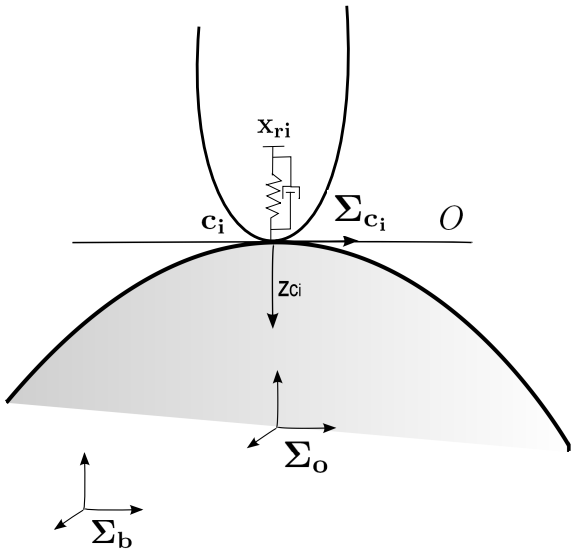

Figure 4.3: Finger in contact with a rigid object. The soft-pad is modeled as a spring and a damper.

workspace, so all the three Cartesian force component can be transferred to the object.

Therefore, the elastic behavior of the soft-pad can be represented as a 3-DOF mechanical spring. The torque about axis z_{ci} can be transferred as well, but this case is not considered here.

Hereafter, for simplicity subscript i is omitted in the discussion.

Let:

$$d\mathbf{p_{c,r}} = \mathbf{p_r} - \mathbf{p_c} \tag{4.17}$$

denote the elementary displacement from the equilibrium of frame $\mathbf{\Sigma}_r$ with respect to frame $\mathbf{\Sigma}_c$.

This elementary displacement (soft-pad flattening) is assumed to be equivalently referred to frame $\mathbf{\Sigma}_r$ or $\mathbf{\Sigma}_c$, because, at the equilibrium, the two frames coincide; therefore, the reference frame was not explicitly denoted. To the displacement $d\mathbf{p_{c,r}}$, coinciding with the deformation of the nonlinear spring of the soft-pad, it corresponds at the equilibrium, the elastic force:

$$\mathbf{F_c} = \mathbf{K_s}\, d\mathbf{p_{c,r}}, \tag{4.18}$$

applied by the finger to the object and referred equivalently to one of the two reference frames.

For the action-reaction law, the force applied by the object to the finger has the expression:

$$-\mathbf{F_c} = \mathbf{K_s} d\mathbf{p_{r,c}}. \tag{4.19}$$

The (3x3) matrix $\mathbf{K_s}$ is the symmetric translational stiffness, that for small displacement can be consider diagonal, whose diagonal elements are the principal translational stiffness, namely, the normal stiffness K_N, and the tangential stiffness K_T.

The tangential component of the contact force is proportional to the tangential flattening of the soft pad trough the nonlinear tangential stiffness, $K_T(\delta_N)$, that depends on the normal displacement of the soft-pad.

Once the desired normal component of the contact force is known from the friction cone condition, and the desired flattering is computed from(4.15), the desired position of the rigid finger is available for the finger control, and can be easily expressed in the palm frame, knowing the thickness of the soft-pad, $\mathbf{t}$, expressed in the contact frame

$$\mathbf{p_{r_d}} = \mathbf{p_c} + \mathbf{R_c}(d\mathbf{p_{c,r}} - \mathbf{t^c}), \tag{4.20}$$

where $\mathbf{R_c}$ is the rotation matrix of frame $\mathbf{\Sigma}_c$, with respect to the palm frame, $\mathbf{\Sigma}_p$, and $\mathbf{p_c}$ is the position of the contact frame in the palm frame.

The cartesian stiffness control, applied to the finger, can be seen as a virtual spring attached to the rigid finger tip.

In this way we have the series of two springs at the contact, the one of the controller and the one of the soft pad. In the range of contact forces that the finger can exert to the object, the stiffness of the soft pad is smaller than the stiffness of the controller.

In this case, the desired position of the rigid fingertip can be achieved with a very small error.

The proposed control law for the hand is obtained stacking the classical proportional action control for each finger. A suitable frame to design the control law can

be the palm frame, $\mathbf{\Sigma}_p$, as done for the arm.

$$\boldsymbol{\tau}_h = \mathbf{K_{P_h}} \mathbf{J_h^T} (\mathbf{p_{r_d}} - \mathbf{p}_\mathrm{e}), \tag{4.21}$$

$\mathbf{J_h}$ is the Jacobian hand matrix and $\mathbf{K_{P_h}}$ is a positive diagonal block matrix, $\mathbf{p_{r_d}} = [\mathbf{p_{r_d}^1}, \ldots, \mathbf{p_{r_d}^n}], \mathbf{p}_\mathrm{e} = [\mathbf{p}_\mathrm{e}^\mathbf{1}, \ldots, \mathbf{p}_\mathrm{e}^\mathbf{n}]$ are the vectors of the desired fingers Cartesian positions and the effective positions respectively, in the palm frame, n is the number of the fingers.

The initial value of the contact forces at the tips for the situation represented in Fig. 4.1 can be computed as follows. Assuming that the object is motionless and in free space, the weight of the object must be balanced by the tangential components of the contact forces, while the normal components to the surface of the object are the internal forces.

If $\hat{\mathbf{h_0}}$ is the estimated gravity vector of the object in the palm frame, the estimated balancing contact force at the fingers are given by the vector

$$\mathbf{F_c} = \mathbf{G_p^\dagger} \hat{\mathbf{h}}_\mathbf{0} + \mathbf{F_N}, \tag{4.22}$$

such as

$$\mathbf{F_T} = \mathbf{G_p^\dagger} \hat{\mathbf{h}}_\mathbf{0}. \tag{4.23}$$

For each finger, by applying the friction cone condition, we compute the norm of the desired initial value of the normal component, F_N, given the tangential component F_T; then, the desired normal flattening of the soft-pad can be expressed as

$$(d\mathbf{p_{c,r}})\hat{\mathbf{n}} = \delta_N = \frac{1}{\nu} \ln(1 + \frac{\nu}{\eta} F_N), \tag{4.24}$$

where $\hat{\mathbf{n}}$ is the unit vector of the normal direction to the object surface in the point of contact.

From this equation, the initial value of the controller set point $\mathbf{p_{r_d}}$, can be computed by substituting(4.24) in(4.20).

During the interaction, the set point is update considering the normal and tangential component of the contact forces measured, and augmenting the normal component of a certain rate, chosen empirically, until condition(4.14) is fulfilled.

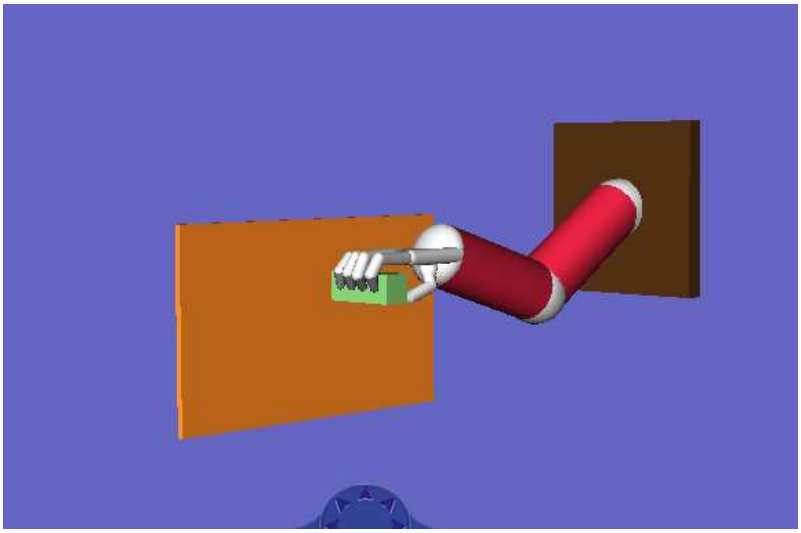

Figure 4.4: Rendering of the hand-arm-object system when the interaction with the elastic environment occur.

4.3 Simulations

A simple case study is considered, where a 5-fingers hand grasps a prismatic object. Four fingers are applied to one side of the object and the thumb to the opposite side. The contact points on the object lie in the same plane passing trough the center of mass of the object and parallel to the base side, so that, in the absence of motion, the resultant force and resultant moment on the object due to the normal component exerted by the fingers are null. The fingers are already in contact with the object. This condition is not restrictive, since the arm and hand controller are designed to be effective even during pre-grasping phase. It is assumed that, during the motion, the object comes in contact with a human, modeled as an elastic environment, see Fig 4.4.

During the execution of the desired trajectory, when the object move in the free space, the controller of the arm guarantees tracking of the desired motion of the object in the work space; in the mean time, the hand controller imposes the contact force necessary to balance the weight of the object with a certain safety factor.

When the object interact with the human, an external force is applied to the object. The hand controller increases the contact forces so that the object is not lost. The compliance behavior of the arm ensures a limited interaction force between

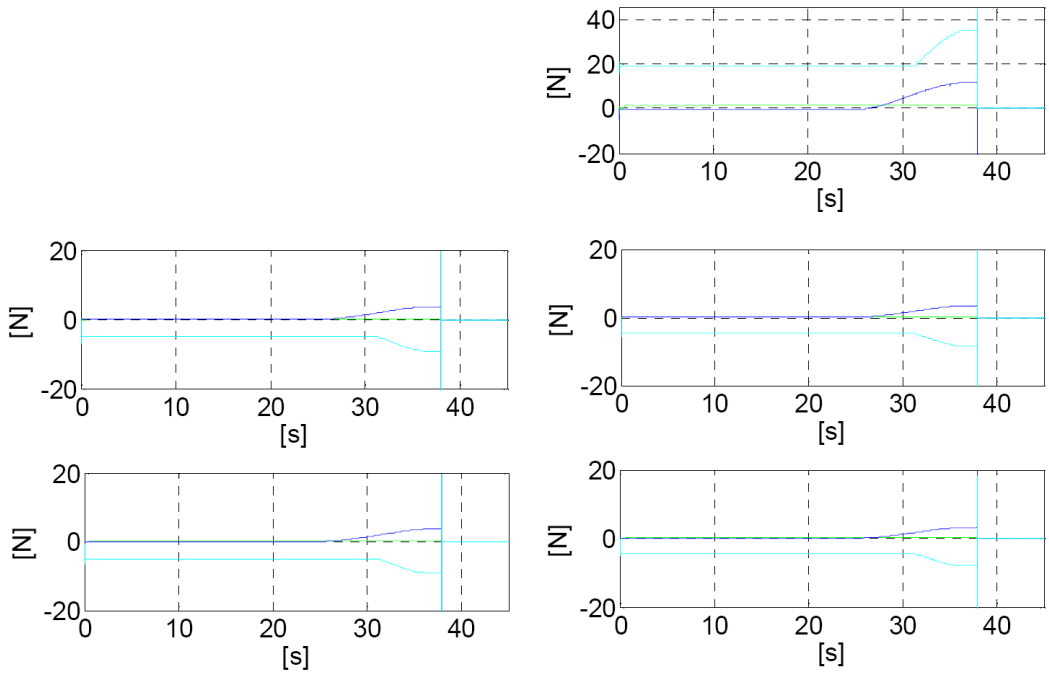

Figure 4.5: Time histories of the contact forces for the five fingers in the case of control law (4.1). The plot on the top corresponds to the thumb.

the object and the environment.

4.3.1 Simulation Software Description

A detailed simulation model of the DEXMART UB Hand III has been developed, based on SimMechanics toolbox of MATLAB.

The hand is constituted by five identical fingers. Each finger is characterized by 4 joints and a coupling between the movements of the last two joints, similarity to the human hand. Hence, only 16 DOF's of the hand are linear independent.

An anthropomorphic arm with seven DOF's has been considered. The dynamics and the kinematics of the 5 fingers and the arm are modeled and simulated in SimMechanics software, using a suite of tools to specify bodies and their mass properties, their possible motions, kinematic constraints, and coordinate systems. Connecting SimMechanics blocks to normal Simulink blocks through sensor and ac-

tuator blocks is possible to control in real time a complex mechanical model and to connect independent mechanical components, like hand/arm system and object, so that they share same mechanical environment. Measures of body motions are available. The coordinate transformations between the base frames of the five fingers and the palm frame is constant.

A block computing contact forces exchanged between the fingers and the object, depending on the behavior of the soft-pads and on the relative motion between the object and the fingertips, and a block of the object simulation model has been included.

4.3.2 Results

In the first simulation the control law (4.1) is used for the arm, with a high value of $\mathbf{K_P}$, to achieve good position accuracy.

When the interaction of the object with the environment occur, an adjoint external force act on the object causing a deviation of the palm from the desired trajectory. The arm control system reacts to reduce such deviation leading to a build-up of the contact force. On the other hand, the controller of the hand tries to regulate the forces at the contacts to fulfill the friction cone conditions. The hand control works until the saturation of the soft-pads is reached, i.e. the contact becomes rigid. When the external force on the object become too hight with respect to the joint torque limits of the fingers, the hand looses the object.

In Figure 4.5, the time histories of the contact forces at the fingertips are reported. The plot on the top corresponds to the thumb. When the object hits the virtual wall, the contact force starts to increase until saturation is reached and objet is lost. On the top of Figure 4.6 is reported the time histories of the normal and tangential flattering of the soft-pad, on the bottom is represented the friction cone condition that is equal for each finger and is fulfilled when the output signal is equal to one. When the object hits the virtual wall the hand provide to increase the normal flattening of the pad to achieve a higher normal contact force component. At the same time the tangential flattening decrease due to the soft pad material properties. Nevertheless, this is not enough to ensure the grasp stability, due to the stiff behavior of the arm. Using the active compliance control law (4.6), the

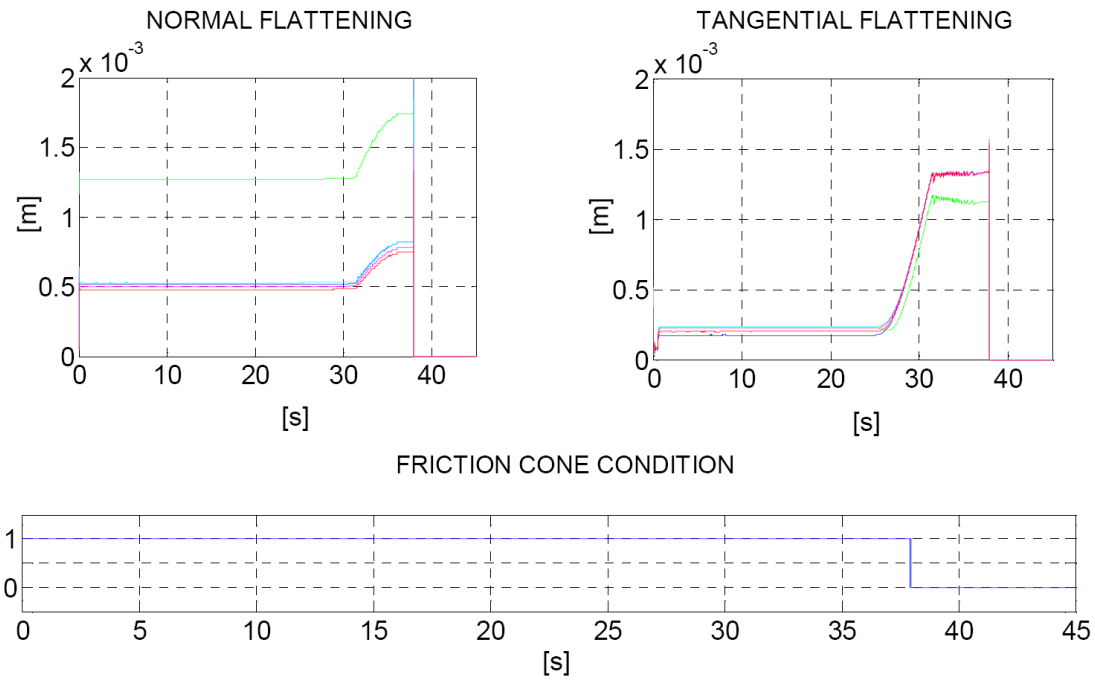

Figure 4.6: The figure represents on the top the graphics of the normal and tangential flattening of the soft-pad for the 5-fingers in the case of stiff behavior of the arm, on the bottom the friction cone condition equal for each finger.

interaction forces with the environment and the contact forces at the fingertip are kept limited. Hence, the hand is able to produce the grasping forces required to fulfill the friction cone condition, also during the interaction with the environment, as we can observe in Fig. 4.7. In Fig. 4.8 histories of the normal and tangential flattening of the soft-pad in the case of compliant behavior of the arm is reported. In Figs. 4.9 and 4.10, the time histories of the error between the desired and actual position trajectory of the palm are reported. When the active compliance control law is applied to the arm, as expected, a relevant position error of the object in the direction of the interaction force with the environment can be observed.

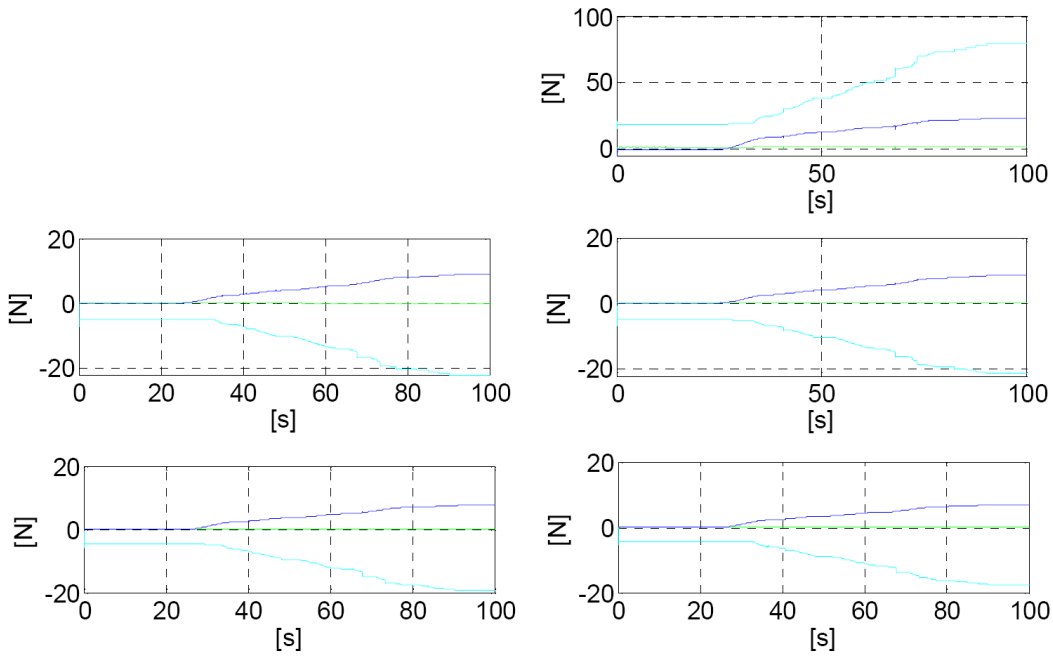

Figure 4.7: Time histories of the contact forces for the five fingers in the case of control law (4.6). The plot on the top corresponds to the thumb.

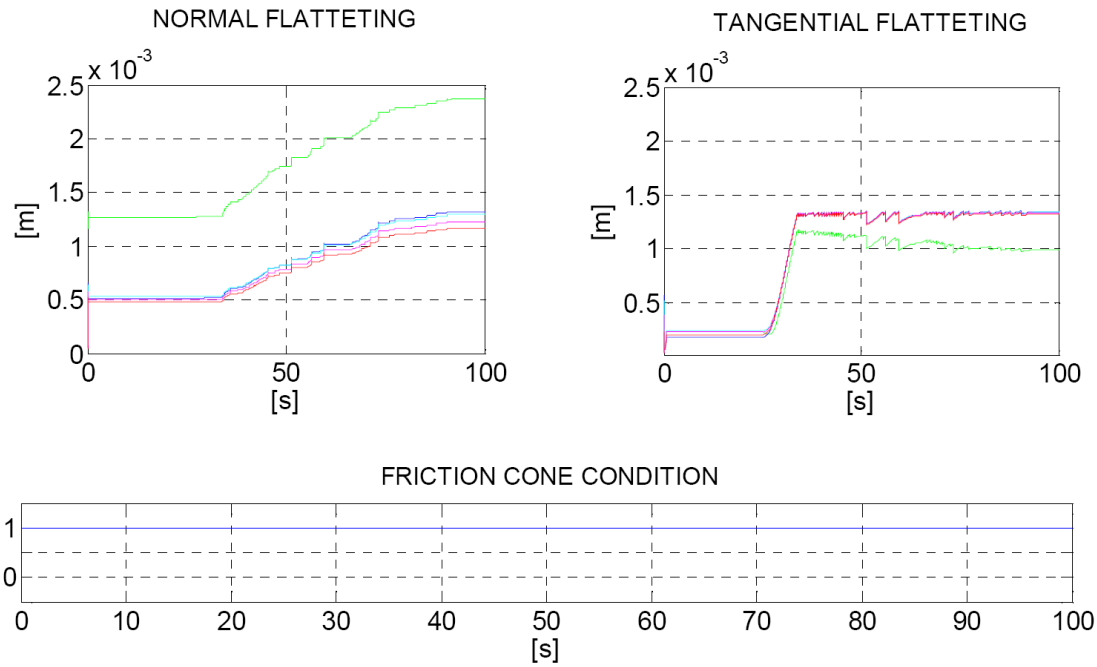

Figure 4.8: The figure represents on the top the graphics of the normal and tangential flattening of the soft-pad for the 5-fingers in the case of compliance behavior of the arm, on the bottom the friction cone condition equal for each finger.

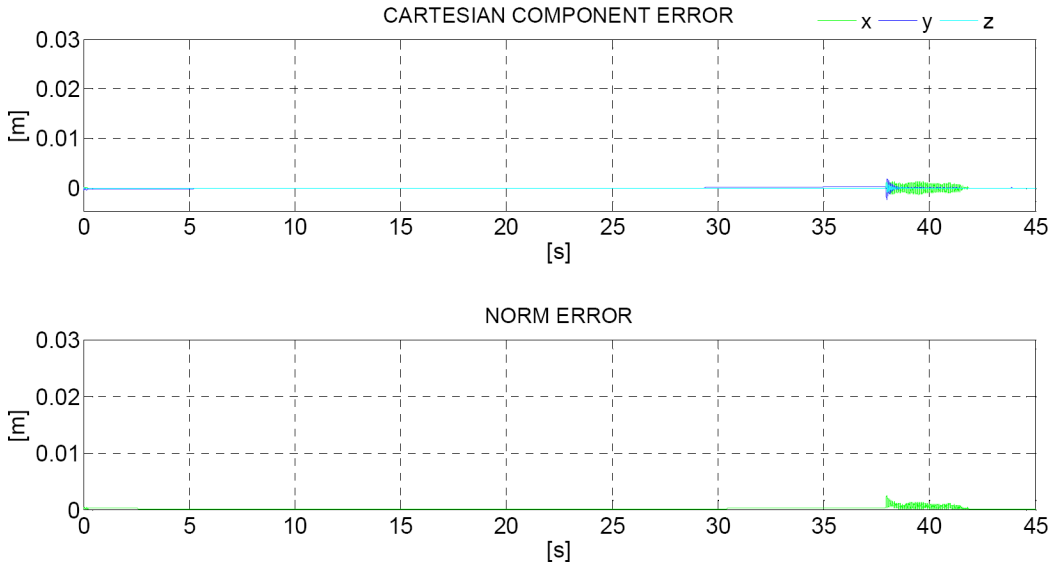

Figure 4.9: The figure represents the Cartesian component error and the norm error related to the palm trajectory, in the case of stiff behavior of the arm.

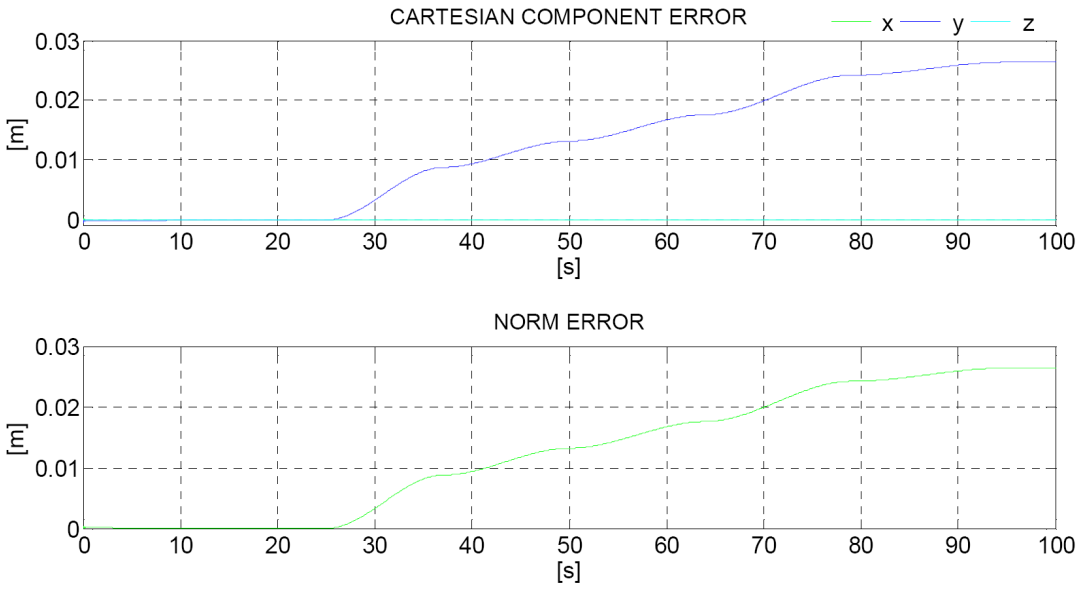

Figure 4.10: The figure represents the Cartesian component error and the norm error related to the palm trajectory, in the case of compliance behavior of the arm.

Chapter 5

Conclusions and Future Researches

5.1 Conclusions and results

The two most distinguished features of humans among animals are hand and mind. Since the next generation of robots will interact with people directly, the interest on the implementation of artificial systems to replicate the manipulating ability of the human hand is growing among researchers. The hand are the interface between the robot and the environment, therefore dexterous manipulation skills are necessary for introduce robot in every day life.

The three most important functions of the human hand are to explore, to restrain (grasping), and to precisely move objects (dexterous manipulation). The work in robot hands has mostly tried to understand and to emulate the last two functions.

The contributions presented in this thesis are aimed at modelling and controlling multi-fingered robotic hands with soft covers for manipulation tasks, essentially for grasping tasks.

5.1.1 Modelling in port-Hamiltonian framework

In this work, a port-Hamiltonian analysis and model of a multi-fingered robotic hand with soft-pads while grasping and manipulating an object, is presented.

The main advantage of this formalism is that it allows to describe the behavior

of the system in terms of energy storage and energy flow, using the concept of power ports. This formalism represents an efficient and useful way to describe the interaction between the object and the fingers, as well as the interaction of the whole system with the environment.

The viscoelastic description of the contact can be expressed in terms of energy storage and dissipation element as a power continuous interconnection, represented by a Dirac structure. Therefore, we are able to describe non-contact to contact transition, and contact viscoelasticity without changing the dynamical equations of the model.

The use of port-Hamiltonian method may be interesting for high-level control problems and where is expected the interact with the environment, since the study can be addressed more intuitively using the concept of passivity. For a complex robotic systems such as the UB hand III actuated by means of tendons and involving considerable problems of friction and elasticity, the use of this tool can be complicated and difficult to implement. Thus for modeling and control complex robotic system the classical Lagrangian method is preferable.

5.1.2 Impedance Hand-Arm control

A control law for a hand-arm system with soft fingers is proposed. During the task execution, interaction of the grasped object with the environment can occur, due to unexpected obstacles or to a pre-planned interaction with a human being.

For control purposes, the hand and the arm are considered as two separate subsystems. The action of the external forces on the object can lead to hight contact forces. To deal with this problem, the control law used for the arm is a compliance object-level control strategy, which aims at controlling the motion of the object and reducing the interaction forces with the environment.

These forces are reconstructed on the basis of the force sensor measurements at the fingertips. The regulation of the contact forces, to guarantee the stability of the grasp and its feasibility, is relegated to the hand control.

Keeping a separate control law for the arm and the hand leads to a better regulation of the internal grasping forces, which is in the charge of the finger control, while the interaction of the object with the environment or a human being is managed

only by the arm control.

A detailed simulation model of the robotic arm-hand-object has been developed with the aim of testing suitable control strategies.

5.2 Ideas for future researches

About modelling and control of a multifingered robotic hand with soft covers in port-Hamiltonian framework, future work will focus on the passive control of the internal and external forces, also in case of sharing tasks with a human being [60]. Moreover, different models of the soft-pad will be used, like soft-pads with nonlinear stiffness [6].

In the case of the whole hand/arm control using soft covers for the hand, future work will focus on the control of a two hand/arm system in bimanual manipulation and cooperative tasks with human beings. A crucial point will be the distribution of the impedance in the whole hand/arm system and between the two arms. Moreover an investigation of human-like behaviors to set the impedance parameters will be evaluated. Those studies, applied to complex systems where actuation by means of tendons occurs, will be conducted with the Lagrangian formalism.

Bibliography

[1] A. Cavallo and G. De Maria and C. Natale and S. Pirozzi, *Optoelectronic joint angular sensor for robotic fingers*, Sensors and Actuators A: Physical **152** (2009).

[2] R. O. Ambrose, H. Aldridge, R. S. Askew, R. R. Burridge, W. Bluethmann, M. Diftler, C. Lovchik, D. Magruder, and F. Rehnmark, *Robonaut: Nasa's space humanoid*, IEEE Intelligent System (2000).

[3] B. Siciliano and O. Khatib (Eds.), *Springer Handbook of Robotics*, ch. 28, Grasping.

[4] J.-H. Bae, S. Arimoto, R. Ozawa, M. Sekimoto, and M. Yoshida, *A unified control scheme for a whole robotic arm-fingers system in grasping and manipulation*, IEEE International Conference on Robotics and Automation (2006).

[5] G. Berselli, G. Borghesan, M. Brandi, C. Melchiorri, C. Natale, G. Palli, S. Pirozzi, and G. Vassura, *Integrated mechatronic design for a new generation of robotic hands*, 8th IFAC International Symposium on Robot Control (2009).

[6] G. Berselli and G. Vassura, *Differentiated layer design to modify the compliance of soft pads for robotic limbs*, IEEE International Conference on Robotics and Automation (2009).

[7] L. Biagiotti, *Advanced Robotic Hands: Design and Control Aspects*, Ph.D. thesis, Università Degli Studi di Bologna, 2002.

[8] L. Biagiotti, F. Lotti, C. Melchiorri, P. Tiezzi, and G. Vassura, *UBH III: An anthropomorphic hand with simplifed endo-skeletal structure and soft continuous fingerpads*, IEEE International Conference on Robotics and Automation (2004).

[9] L. Biagiotti, C. Melchiorri, P. Tiezzi, and G. Vassura, *Modelling and identification of soft pads for robotic hands*, IEEE/RSJ International Conference on Intelligent Robots and Systems (2005).

[10] L. Biagiotti, P. Tiezzi, C. Melchorri, and G. Vassura, *Modelling and controlling the compliance of a robotic hand with soft finger-pads*, IEEE International Conference on Robotics and Automation (2004).

[11] A. Bicchi, *Hands for dexterous manipulation and robust grasping: A difficult road toward simplicity*, IEEE Trans. Robot. Automat. **16** (2000), no. 6, 652–662.

[12] G. Borghesan, G. Palli, and C. Melchiorri, *Design of tendon-driven robotic fingers: Modelling and control issues*, IEEE International Conference on Robotics and Automation (2010).

[13] P.C. Breedveld, *Physical Systems Theory in Terms of Bond Graphs*, Ph.D. thesis, University of Twente, Enschede, 1984.

[14] J. Butterfass, M. Grebenstein, H. Liu, and G. Hirzinger, *Dlr-hand II: Next generation of a dextrous robot hand*, Proc. IEEE International Conference on Robotics and Automation.

[15] Controllab Products B.V., *20-sim*, http://www.20sim.com (2009).

[16] A. Caffaz and G. Cannata, *The design and development of the dist-hand dextrous gripper*, IEEE International Conference on Robotics and Automation (1998).

[17] R. Cassinis, *Robotica avanzata: Una allettante prospettiva di sviluppo*, www.ing.unibs.it/ arl/docs/papers.

[18] A. Cavallo, G. De Maria, C. Natale, and S. Pirozzi, *Minimally invasive force sensing for tendon-driven robots*, Cutting Edge Robotics 2009, IN-TECH Online (2009).

[19] M. R. Cutkosky, J. M. Jourdain, and P. K. Wright, *Skin materials for robotic fingers*, IEEE Int. Conf. on Robotics and Automation (1987).

[20] M. R. Cutkosky and P. K. Wright, *Friction, Stability and the Design of Robotic Fingers*, The International Journal of Robotics Research **5** (1986), no. 4, 20–37.

[21] C. Canudas de Wit, H. Olsson, K. J. Åström, and P. Lischinsky, *A new model for control of systems with friction*, IEEE Transactions on Automatic Control **40** (1995).

[22] Scuola di Robotica Home Page, *http://www.scuoladirobotica.it*.

[23] N. Diolaiti, C. Melchorri, and S. Stramigioli, *Contact impedance estimation for robotic systems*, IEEE Trans. on Robotics **21** (2005).

[24] S.C. Jacobsen et al., *Design of the utah/mit dexterous hand*, Proc. IEEE International Conference on Robotics and Automation.

[25] F. Ficuciello, R. Carloni, L. C. Visser, and S. Stramigioli, *Port-Hamiltonian Modelling for Soft-Finger Manipulation*, IROS International Conference on Intelligent Robots and Systems (2010).

[26] F. Ficuciello and L. Villani, *Compliant Hand-Arm Control with Soft Fingers and Force Sensing for Human-Robot Interaction*, Submitted to IFAC International Symposium on Robot Control (2011).

[27] European Seventh Framework Programme for Research and Technology Development (FP7), *http://cordis.europa.eu/fp7*.

[28] N. Fukaya, S. Toyama, T. Asfour, and R. Dillmann, *Design of the tuat/karlsruhe humanoid hand*, Proc. IEEE/RSJ Int.Conf.on Intelligent Robots and Systems (2000).

[29] G. Berselli and G. Vassura, *Tailoring the viscoelastic properties of soft pads for robotic limbs through purposely designed fluid filled structures*, IEEE International Conference on Robotics and Automation (2010).

[30] J.P. Gazeau, S. Zeghloul, M. Arsicualt, and J.P. Lallemand, *The lms hand: force and position controls in the aim of fine manipulation of objects*, Proc. IEEE International Conference on Robotics and Automation.

[31] Barret hand webpage, *http://www.barretttechnology.com*.

[32] Dist hand webpage, *http://www.graal.dist.unige.it/research*.

[33] Robonaut hand webpage, *http://vesuvius.jsc.nasa.gov*.

[34] Shadow hand webpage, *http://www.shadow.org.uk/*.

[35] N. Hogan, *Impedance control: An approach to manipulation: Parts I-III*, ASME Trans. Jour. Dynamic Systems and Measurement Control **107** (1985).

[36] J. Huang, D. Yamada, T. Horiand, M. Hara, and T. Yabuta, *Integration of impedance control and manipulability regulation for a finger-arm robot*, IEEE International Conference on Robotics and Automation (2009).

[37] H. Kawasaki, H. Shimomura, and Y. Shimizu, *Educational-industrial complex development of an anthropomorphic robot hand 'gifu hand'*, Advanced Robotics **15** (2001), no. 3.

[38] K. Lee and I. Shimoyama, *A skeletal framework artificial hand actuated by pneumatic artifcial muscles*, IEEE International Conference on Robotics and Automation (1999).

[39] V. Lippiello, B. Siciliano, and L. Villani, *Real-time dextrous-hand grasping force optimization with dynamic torque constraints*, Submitted to IEEE International Conference on Robotics and Automation (2011).

[40] C.S. Lovchik and M.A. Diftler, *The robonaut hand: a dexterous robot hand for space*, IEEE International Conference on Robotics and Automation (1999).

[41] C. Melchiorri and G. Vassura, *Mechanical and control features of the UB Hand Version II*, Proc.IEEE/RSJ Int.Conf.on Intelligent Robots and Systems.

[42] C. Melchorri and J. Salisbury, *Exploiting the redundancy of a hand-arm robotic system*, MIT, A.I. Memo (1990).

[43] R. Murray, Z. Li, and S.S. Sastry, *A mathematical introduction to robotic manipulation*, CRC Press.

[44] C. Natale and S. Pirozzi, *Minimally invasive torque sensor for tendon-driven robotic hands*, IEEE/RSJ International Conference on Intelligent Robots and Systems (2008).

[45] T. Okada, *Computer control of multijointed finger system for precise object handling*, International Trends in Manufacturing Technology- Robot Grippers (1986).

[46] DEXMART Home Page, *http://www.dexmart.eu/*.

[47] The Hand Embodied Research Project Home Page, *http://www.thehandembodied.eu/project*.

[48] G. Palli, G. Borghesan, and C. Melchiorri, *Tendon-based transmission systems for robotic devices: Models and control algorithms*, IEEE International Conference on Robotics and Automation (2009).

[49] G. Palli and C. Melchiorri, *Model and control of tendon-sheath transmission system*, IEEE Int. Conf. on Robotics and Automation (2006).

[50] S. Pirozzi and L. Grassia, *Tactile sensor based on led-phototransistor couples*, Tactile Sensing Workshop, 9th IEEE-RAS International Conference on Humanoid Robots (2009).

[51] S. Stramigioli and V. Duindam, *Modelling the kinematics and dynamics of compliant contact*, IEEE International Conference on Robotics and Automation (2003).

[52] S. Stramigioli and V. Duindam, *Port Based Modelling of Spatial Visco-Elastic Contacts*, European Journal of Control **34** (2004), no. 2, 510–519.

[53] K.S. Salisbury and B.Roth, *Kinematics and force analysis of articulated mechanical hands*, Journal of Mechanims, Transmissions and Actuation in Design (1983).

[54] M. Santello, M. Flanders, and J.F. Soechting, *Postural hand synergies for tool use*, The Journal of Neuroscience **18** (1998), no. 23, 10105–10115.

[55] S. Schulz, C. Pylatiuk, and G. Bretthauer, *A new ultralight anthropomorphic hand*, Proc. IEEE International Conference on Robotics and Automation (2001).

[56] K. B. Shimoga and A. A. Goldenberg, *Soft Robotic Fingertips: Part I: A Comparison of Construction Materials*, The International Journal of Robotics Research **15** (1996), no. 4, 320–334.

[57] B. Siciliano and O. Khatib (Eds.), *Springer handbook of robotics*, ch. 15, Robot Hands.

[58] B. Siciliano, L. Sciavicco, L. Villani, and G. Oriolo, *Robotics Modelling, Planning and control,Springer*, Springer, London, UK.

[59] S. Stramigioli, *Modelling and IPC Control of Interactive Mechanical Systems: A Coordinate-free Approach*, Springer-Verlag.

[60] S. Stramigioli and V. Duindam, *Variable Spatial Springs for Robot Control*, IEEE/RSJ Int. Conf. on Intelligent Robots and Systems (2001).

[61] A.J. van der Schaft, *L_2-Gain and Passivity Techniques in Nonlinear Control*, Springer.

[62] A.J. van der Schaft and B.M. Maschke, *On the Hamiltonian formulation of nonholonomic mechanical systems*, Reports on Mathematical Physics **34** (1994), no. 2, 225–233.

[63] Official Roboethics Website, *http://www.roboethics.org*.

[64] T. Wimboeck, C. Ott, and G. Hirzinger, *Impedance behaviors for two-handed manipulation: Design and experiments*, IEEE International Conference on Robotics and Automation (2007).

[65] W.T.Townsend, *Mcb - industrial robot feature article- barrett hand grasper*, Industrial Robot: An International Journal **3** (2000), no. 27.

[66] T. Wurtz, C. May, B. Holz, C. Natale, G. Palli, C. Melchiorri, and G. Vassura, *The twisted string actuation system: Modelling and control*, IEEE/ASME International Conference on Advanced Intelligent Mechatronics (2010).

[67] M. Zefran and V. Kumar, *Affine connections for the Cartesian stiffness matrix*, IEEE International Conference on Robotics and Automation (1997).